Report Number NPS-69-82-007

# NAVAL POSTGRADUATE SCHOOL

## Monterey, California


ADVANCED COMPOSITES FIRE RESPONSE PROGRAM

by

David Salinas and Costa Vatikiotis

Progress Report for Period
October 1981 - September 1982



Prepared for: Naval Weapons Center
China Lake, CA 93555

NAVAL POSTGRADUATE SCHOOL
Monterey, California

J. J. Ekelund, RADM, USN
Superintendent

D. A. Schrady
Provost

This report documents progress for the period ending 30 September 1982 in the analytical investigation of the effects of a severe thermal environment on composite laminates of the project titled "Advanced Composites Fire Response Program."

The work reported herein has been monitored and supported by the Naval Weapons Center, China Lake, CA 93555.



This report was prepared by:

UNCLASSIFIED
SECURITY CLASSIFICATION OF THIS PAGE (When Data Entered)

| REPORT DOCUMENTATION PAGE | | READ INSTRUCTIONS BEFORE COMPLETING FORM |
|---|---|---|
| 1. REPORT NUMBER<br>NPS-69-82-007 | 2. GOVT ACCESSION NO. | 3. RECIPIENT'S CATALOG NUMBER |
| 4. TITLE (and Subtitle)<br>ADVANCED COMPOSITES FIRE RESPONSE PROGRAM | | 5. TYPE OF REPORT & PERIOD COVERED<br>Progress October 81-Sept 82 |
| | | 6. PERFORMING ORG. REPORT NUMBER |
| 7. AUTHOR(s)<br>David Salinas and Costa Vatikiotis | | 8. CONTRACT OR GRANT NUMBER(s) |
| 9. PERFORMING ORGANIZATION NAME AND ADDRESS<br>Naval Postgraduate School<br>Monterey, CA 93940 | | 10. PROGRAM ELEMENT, PROJECT, TASK AREA & WORK UNIT NUMBERS<br>63262N: W01088<br>N6053082WR30093 |
| 11. CONTROLLING OFFICE NAME AND ADDRESS<br>Naval Weapons Center<br>China Lake, CA 93555 | | 12. REPORT DATE<br>September, 1982 |
| | | 13. NUMBER OF PAGES<br>58 |
| 14. MONITORING AGENCY NAME & ADDRESS(if different from Controlling Office) | | 15. SECURITY CLASS. (of this report)<br>Unclassified |
| | | 15a. DECLASSIFICATION/DOWNGRADING SCHEDULE |

16. DISTRIBUTION STATEMENT (of this Report)

Approved for Public Release: Distribution Unlimited

17. DISTRIBUTION STATEMENT (of the abstract entered in Block 20, if different from Report)

18. SUPPLEMENTARY NOTES

19. KEY WORDS (Continue on reverse side if necessary and identify by block number)

Composites, Thermal Behavior, Strength Analysis

20. ABSTRACT (Continue on reverse side if necessary and identify by block number)

This report discusses the status of an analytical investigation of the effects of a severe thermal environment on composite laminates. Models for the thermal and strength behavior have been developed. Some results of computer analyses are reported.

DD FORM 1 JAN 73 1473 EDITION OF 1 NOV 65 IS OBSOLETE
S/N 0102-014-6601

UNCLASSIFIED
SECURITY CLASSIFICATION OF THIS PAGE (When Data Entered)

TABLE OF CONTENTS


List of Figures and Tables.....iv
1.0 Introduction.....1
2.0 Thermal Investigation.....3
2.1 Objectives.....3
2.2 Description of the Model.....3
2.3 Generalization of the Model.....6
2.3.1 Modularization of the Computer Program.....6
2.3.2 Transient Porosity and Permeability.....7
2.3.3 Combustion.....7
2.3.4 Arrhenius Expression.....7
2.3.5 Transient Plate Thickness.....8
2.3.6 Porous Model.....8
2.3.7 Heat Transfer Coefficient.....8
2.3.8 Surface Recession Problem.....8
2.3.9 Initial Conditions.....9
2.3.10 Boundary Conditions.....9
2.3.11 Numerical Instabilities.....9
2.3.12 Improved Accuracy.....9
2.3.13 Updating Thermophysical Properties.....10
2.3.14 Thermal Conductivity.....10
2.4 Dissertation Results.....10
2.4.1 Effects of Fire Environment.....11
2.4.2 Effects of Permeability.....21
2.4.3 Effects of Porosity.....24
2.4.4 Effects of Thickness.....24
2.4.5 Effects of Pressure Differental.....29
2.4.6 Effects of Boundary Conditions.....30
2.4.7 Effects of Pore Velocity.....34
2.5 NPS Activity.....34
2.5.1 Restart Capability.....34
2.5.2 Effects of Initial Conditions.....36
2.5.3 Graphics Capability.....38
3.0 Strength Investigation.....52
3.1 Objectives.....52
3.2 Description of the Model.....52

3.3 Modifications of the Model.....53
3.3.1 Nonsymmetric Temperature Fields.....53
3.3.2 Additional Failure Factors.....54
3.4 Sample Analysis.....55
References.....57

LIST OF FIGURES AND TABLES


Figure 1 Geometry of the Model.....5
Figure 2 Comparison of Experimental and Analysis Results..13
Figure 3 Temperatures for Fire Environment Study.....16
Figure 4 Concentration for Fire Environment Study.....17
Figure 5 Thickness for Fire Environment Study.....18
Figure 6 Temperatures for Fire Environment Study.....19
Figure 7 Concentration for Fire Environment Study.....20
Figure 8 Temperatures for Permeability Study.....23
Figure 9 Temperatures for Porosity Study.....26
Figure 10 Temperatures for Thickness Study.....28
Figure 11 Temperatures for Pressure Differential Study.....32
Figure 12 Temperatures for Boundary Condition Study.....33
Figure 13 Temperatures versus Filter Velocity.....35
Figure 14 Temperatures for Initial Condition Study.....37
Figure 15 Temperature Surface from GRAF3D.....40
Figure 16 Concentration Surface from GRAF3D.....41
Figure 17 Reaction Rate Surface from GRAF3D.....42
Figure 18 Temperature Contours from GRAF3D.....43
Figure 19 Concentration Contours from GRAF3D.....44
Figure 20 Reaction Rate Contours from GRAF3D.....45
Figure 21 Subregion Surface of Figure 15.....46
Figure 22 Subregion Surface of Figure 16.....47
Figure 23 Subregion Surface of Figure 17.....48
Figure 24 Subregion Contour of Figure 18.....49
Figure 25 Subregion Contour of Figure 19.....50
Figure 26 Subregion Contour of Figure 20.....51
Figure 27 Failure Locus for 0/90 Graphite-Epoxy Laminate...56

Table 1 Data for Experimental-Analysis Comparison.....12
Table 2 Data for Fire Environment Study.....15
Table 3 Data for Permeability Study.....22
Table 4 Data for Porosity Study.....25
Table 5 Data for Thickness Study.....27
Table 6 Data for Pressure Differential Study.....31

# chapter 1
# INTRODUCTION

This report describes the status of an investigation into the behavior of a composite structure in a fire environment. The investigation arises from the need to assess the damage a composite aircraft structure undergoes when exposed to a carrier deck pool fire. Towards this end, the Naval Weapons Center (NWC) in China Lake has undertaken a series of experiments to determine the effects of fires on structures (1). As the number of parameters effecting thermal behavior is large, and as the behavior is inherently nonlinear, an exhaustive experimental study is prohibitive in cost and time. To assist their experimental program, NWC has funded the NAVAL POSTGRADUATE SCHOOL (NPS) to develop a mathematical model of the problem. The NWC experimental investigation, and the NPS analytical investigation are intended to complement one another.

The NPS effort seeks to quantitatively predict the extent of damage a composite structure undergoes when exposed to a fire. This objective was to be achieved through the development of a mathematical model of the problem. The computer program resulting from the mathematical model would be used to predict the thermal behavior of composites for a wide range of system parameters. The parameters characterizing a system include (1) composite components (materials), (2) composite layup (lamina orientation), (3) composite thickness, (4) permeability, (5) porosity, (6) wind, and (7) fire intensity. The degree of validity of the model could be established by comparing the results of the model to experimental results. Moreover, the model would be used to suggest the most appropriate experiments.

The overall problem of the behavior of a composite in a fire environment is conveniently partitioned into two investigations; an investigation of thermal behavior, and an

investigation of how composite strength is affected by it's temperature distribution.

Mathematical models of both thermal behavior and strength behavior have been developed. The computer codes resulting from the mathematical models have been implemented on a number of cases. Some results and brief descriptions of the thermal and strength analyses follow.

# chapter 2
# THERMAL INVESTIGATION

The thermal investigation is concerned with the determination of the temperature profile in a composite laminate due to exposure to a fire environment.

## 2.1 OBJECTIVES

The objectives of the thermal investigation are:

1. development of a mathematical model for the determination of behavior of a composite laminate in a fire environment.
2. to show how each of the system parameters affect the thermal behavior.
3. to evaluate the extent, and rate of material consumption due to combustion.
4. to extend the Semenov combustion model to composite media.

## 2.2 DESCRIPTION OF THE MODEL

The principal investigator for the determination of thermal response of a composite laminate in a fire environment, until the receipt of his Doctoral Degree in June 1982, has been Lcdr. C.S. Vatikiotis of the U.S. Navy. Initally Lcdr. Vatikiotis (then a Lieutenant) worked on the problem to satisfy the research requirement towards an Engineer's Degree in Mechanical Engineering from NPS. The degree was granted in June 1980. A brief description of the mathematical model for the thermal behavior follows. A more detailed description is contained in references (2,3).

We consider a composite of graphite fibers imbedded in an epoxy matrix. As epoxy combusts at a much lower temperature

than graphite, the model assumes the epoxy has burnt off and all that remains is a porous graphite medium. Figure 1 presents a diagram of the geometry of the porous medium. A pressure differential across the porous plate induces an air flow through the medium. The air flow provides two opposing actions; heat generation and heat transfer. The heat generation results from the combustion which requires oxygen to be ever present. Heat is transferred through the porous medium by convective air flow. Behavior of the system depends upon which of these effects, heat generation or heat transfer, dominates.

A one dimensional model of a porous medium was developed on the basis of the following fundamental laws:

1. an energy balance on the graphite,
2. an energy balance on the air, and
3. a mass balance on the oxygen.

All of the heat transfer modes, conduction, convection, and radiation are included in the model. In addition, the energy balance equation for the graphite contains a heat generation term of Arrhenius type arising from combustion of the graphite. Similarly, the oxygen mass balance equation contains a term accounting for the consumption of oxygen due to combustion.

In addition to the energy and mass balance equations, Darcy's law for the governing equation for air flow through the porous graphite plate was combined with Bernoulli's equation to yield an equation for the pressure differential. As very large changes in temperature occur during the transient history of the system, all thermophysical properties are treated as temperature (and hence time) dependent. The combustion model was patterned after the Semenov model, and the reaction was taken as producing only carbon dioxide.

The mathematical model of the thermal problem consists of three nonlinear, coupled, partial differential equations in time and space. These field equations were transformed, via a Galerkin formulation of the finite element method, into a set of 3xn nonlinear, coupled ordinary differential equa-

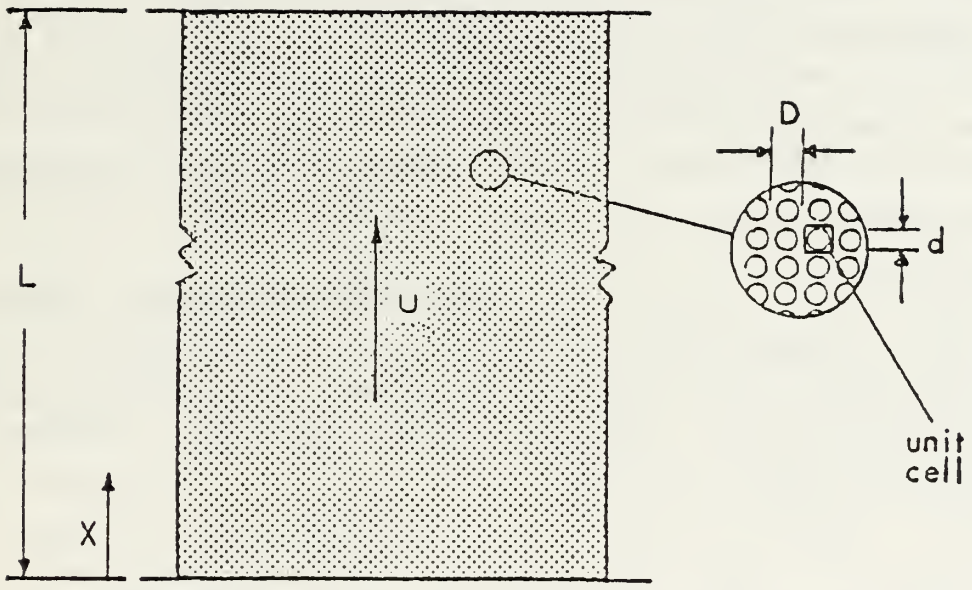


Figure 1. Geometry of the Model

tions in time, where n is the number of spatial nodes in the finite element discretization. These equations, upon numerical integration by the Franke (4) modified Gear method for stiff systems, gives the graphite temperature, the air temperature, and the oxygen concentration at each nodal point as a function of time. In addition to these response variables, a large number of other system parameters are calculated. These include air density, porosity, permeability, Reynold's number, pore velocity, and pressure. In this way a full characterization of the system is known during the transient history of the problem.

## 2.3 GENERALIZATION OF THE MODEL

On the basis of his NPS research activity, Lcdr. Vatikiotis was accepted to the NPS Doctoral program. He was permitted to conduct the research required for the Doctoral Degree at his next duty station, the David Taylor Naval Ship Research and Development Center (NSRDC). During the period of June 1980 to June 1982, Lcdr. Vatikiotis made significant improvements to the thermal model, and performed a number of computer runs to determine the effects of design and environmental parameters on system behavior. A brief description of his work is presented here. For a more detailed account of the work, the reader is referred to the Doctoral dissertation (5).

### 2.3.1 Modularization of the Computer Program

The computer program generated in the Engineer's Degree research effort was put into modular form in order to more easily accommodate any changes to the model. At present, the computer code consists of 25 subroutines.

### 2.3.2 Transient Porosity and Permeability

In the earlier model, porosity and permeability were treated as uniform through the medium, and constant with respect to time. The model was updated to account for an ini-

tial non uniform distribution of graphite filaments. Moreover as graphite is consumed by combustion, both the porosity distribution and permeability distribution vary with time and position. The model was modified to account for the changing air density, and porosity by invoking the continuity equation. Combining the continuity equation with Darcy's law resulted in a fourth nonlinear second order field equation. This equation was solved numerically by the "shooting method".

### 2.3.3 Combustion

In the earlier model the product of the graphite combustion was assumed to be carbon dioxide only (i.e., a simple reaction). The literature shows that carbon monoxide becomes a byproduct, along with carbon dioxide, at higher combustion temperatures. An empirical relation for the proportion of CO and CO2 as a function of temperature was incorporated into the model.

### 2.3.4 Arrhenius Expression

As Frank-Kamenetskii (6) suggested that carbon combustion is not a first order reaction, the model was generalized to accommodate fractional order reactions. This modification was accomplished by raising the oxygen concentration term in the reaction rate expression to a fractional power. A series of analyses were performed with fractional exponents 1/2, 2/3, and 3/4. The analytical results changed markedly with exponent. Hence, the accuracy of any analytical model depends on the accuracy of the experimentally derived exponent.

### 2.3.5 Transient Plate Thickness

Accounting for the change in porosity due to graphite consumption also permitted the determination of the laminate thickness with time.

### 2.3.6 Porous Model

Originally, the porous medium was modeled as cylindrical fibers. The model has been modified so that it can treat either spherical particles or cylindrical fibers. This option permits the user to consider the problem of combustion of graphite particles.

### 2.3.7 Heat Transfer Coefficient

Alternate models for internal heat transfer coefficient, surface area per unit volume, and average pore diameter are available for selection of the investigator. In addition, the pore diameter is based on the hydraulic diameter.

### 2.3.8 Surface Recession Problem

In the case of combustion, the reaction invariably moves to the source of the oxygen, namely the air inlet surface. This results from the fact that in a relatively short time, all oxygen in the interior is consumed. Once all of the interior oxygen has been consumed, all subsequent combustion takes place at the air inlet surface where there is always a continuous supply of oxygen. At this stage in the transient history, the problem degenerates into a "surface recession" problem. Since there is no oxygen except at the inlet surface, the oxygen balance equations must be removed from the analysis, otherwise severe numerical difficulties arise. The removal of these equations from the analysis is accomplished automatically in the computer program, so that the user need not be concerned with the transformation to a surface recession problem.

### 2.3.9 Initial Conditions

The arbitrariness of selecting initial conditions was overcome by incorporating into the analysis, a subroutine which generates a transient thermal environment. If the user selects this mode for the initial conditions, a heat flux and it's duration time are specified by the user.

### 2.3.10 Boundary Conditions

The model was given more flexibility for application to a wider class of problems by allowing a choice of boundary conditions. The user may select any of the following three boundary conditions:

1. insulated surfaces and Dankwert's B.C.'s for the air temperature and oxygen concentration.
2. radiation at surfaces and Dankwert's B.C.'s for the air temperature and oxygen concentration.
3. convective and radiative heat transfer at both surfaces, air temperature at inlet surface equal to ambient temperature, oxygen concentration at the inlet surface equal to ambient concentration, and Dankwert's B.C.'s at the exit surfaces.

### 2.3.11 Numerical Instabilities

During certain times in the transient history, numerical instabilities were encountered. This is particularly true when the oxygen concentration is going to zero in the interior of the medium. The numerical instability appears in the results as an oxygen concentration oscillating about zero. A subroutine was added to the program which dampens the oscillation significantly.

### 2.3.12 Improved Accuracy

In the original formulation of the problem, the nonlinear heat generation term was treated as a "forcing" term. A significant reduction in computational effort resulted when this nonlinear term was treated as a part of the field operator. This improvement in computational effort is attributed to the fact that as an operator, the generation term enters the analysis as part of the Jacobian matrix of the system. As the Jacobian matrix plays a prominent role in the numerical integration, it is no wonder that a significant improvement occurs.

### 2.3.13 Updating Thermophysical Properties

In the original formulation, all temperature dependent properties were updated outside of the time integration loop, at the arbitrary discretion of the user. The formulation was modified so that all temperature dependent properties are updated continuously and automatically within the integration loop. The result is improved accuracy and a reduction of computational effort.

### 2.3.14 Thermal Conductivity

The expression for thermal conductivity of the porous medium was changed to one that extended the range of porosities which could be treated. The magnitudes of the internal parameters, such as pore velocity, etc., are checked to verify that the empirical expressions used to calculate these parameters remain valid.

All of the modifications briefly described above had the effect of (1) extending the model to a more general state, (2) provide the analysis with more accuracy, and (3) reduce the computational effort required in the solution of a problem. In the next section some of the results obtained by Lcdr. Vatikiotis are briefly described.

## 2.4 DISSERTATION RESULTS

A number of computer analyses were performed in order to obtain results which would provide some understanding of the effects of each of the system parameters on system behavior. In order to establish the validity of the mathematical model, a comparison of results from computer analyses with experimental results was made whenever possible. In such cases there was fair agreement between analytical and experimental results. There are three reasons why excellent agreement between experimental and analytical results should not be expected. First, combustion experiments by their very nature are difficult to perform and control. Thus there is a large uncertainty in the reported results. The relatively small number of combustion experiments at-

tests to their difficulty. Secondly, there is small likelihood that the values of many system parameters is known to any high degree of certainty. Thus, for example, the exponent on oxygen concentration in the Arrhenius expression has not been accurately determined; and yet a small change in the exponent yields significant changes in the quantitative results. Thirdly, there is the inherent uncertainty associated with every complex mathematical model. Any number of simplifying assumptions are made; and of course there are choices in the selection of competing relations for calculating properties. All of these considerations suggest that the results be regarded as descriptive rather than precise. As none of the analysis results contradicted experimental results, there is confidence that the mathematical model is a good one. Figure 2 presents a comparison of the mathematical model and the experimental results of Kolodstev (7). The data for the analysis is given in Table 1.

A series of computer runs were performed to isolate the effects of a single system parameter on system behavior. A brief description of each of the studies follows. In each case, the boundary conditions with insulated surfaces was used. The numerical results given in this report should be considered approximate rather than precise.

### 2.4.1 Effects of Fire Environment

In this study, the effect of fire intensity on a composite plate was investigated by subjecting a plate to two heat flux conditions. The first heat flux condition results in combustion, and the second heat flux condition results in extinguishment. Table 2 presents the data describing the composite of this study.

When a heat flux of 30,000 Btu/ft-hr is applied to the inlet surface for 15 seconds, and is then removed, the plate undergoes combustion. Figure 3 shows the graphite and air temperatures as functions of space at selected times. Figure 4 plots oxygen concentration versus space at selected times, and Figure 5 shows the thickness of the plate as a

TABLE 1 --- Geometry of porous medium and ambient conditions for simulating Kolodstev's [ 7 ] experiment.

| | |
|---|---|
| • Particle Shape: | spherical |
| • Particle Diameter ( $d$ ): | .126 in |
| Unit Cell Thickness ( $D$ ): | .126 in |
| • Spatial Thickness of Porous Medium ( $L$ ): | 7.5 in |
| Porosity ( $p$ ) | .476 |
| Permeability ( $m$ ) | $.103 \times 10^{-6}$ $ft^2$ |
| Bulk Thermal Conductivity of Carbon ( $k_c$ ): | 86.0 Btu/ft-hr-F |
| Bulk Specific Heat of Carbon ( $C_c$ ): | .231 Btu/lbm-F |
| Bulk Density of Carbon ( $\rho$ ): | 70.3 $lbm/ft^3$ |
| Thermal Emissivity of Particles ( $\epsilon$ ): | .9 |
| Ambient Temperature ( $T_\infty$ ): | 80.0 deg-F |
| • Ambient Pressure ( $P_\infty$ ): | 14.7 psi |
| • Pressure Differential ( $\Delta P$ ): | -.29 psi |
| • Ambient Oxygen Concentration ( $\phi_\infty$ ): | .0172 $lbm/ft^3$ |

• Known parameter for Kolodstev's experiment.

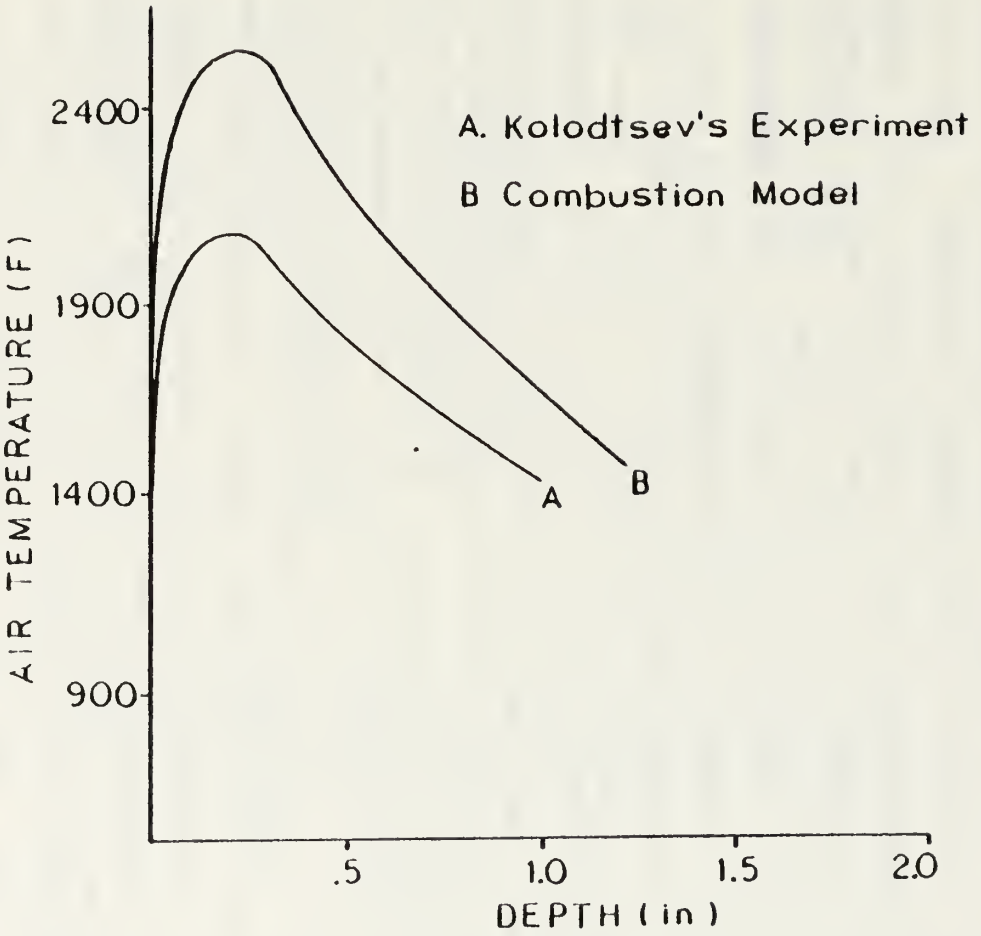


FIGURE 2 --- Air temperature from combustion model shown with that obtained from Kolodstev's [7] experiment.

function of time. Figure 4 shows that the graphite and air temperatures differ only at the air inlet surface (X/L=0.) until about t=360 sec. Thereafter the air temperature is significantly less than the graphite temperature for a considerable range of X/L. This can be misleading because the thickness L has changed significantly during the evolution. Figure 5 shows that the plate thickness at 517 seconds is only 10 percent of it's original thickness. Thus the penetration of "cooler" air is .0025 inches. At 20 seconds, the plate thickness is .25 inches and the cooler air penetrates the plate to X/L=0.1, or .025 inches. Thus when looking at Figure 3, one must keep in mind that L, the thickness of the plate, is changing due to combustion.

An important observation which can be made for this combustion case comes from Figure 4. Figure 4 shows that the oxygen in the interior of the plate is very quickly consumed. All cases which have gone to combustion have shown this trait, the interior oxygen is quickly depleted. At time equal to 20 seconds, the problem is about to become a "surface recession" problem, in which all reaction takes place at the air inlet surface. Figure 5 shows that the rate of material consumption becomes ever increasingly greater with time after surface recession begins. For this particular case we note that the temperature increased from a maximum of 900 degrees Fahrenheit when the heat flux was removed to a temperature slightly less than 3000 degrees Fahrenheit at 517 seconds.

When a heat flux of 30,000 Btu/ft-hr is applied to the inlet surface for 14 seconds and then removed, the plate goes to extinction in less than a minute. Figure 6 shows the manner in which the temperature distribution goes to the uniform ambient temperature. We note that the peak temperature while continuously decreasing in magnitude with time, moves from the inlet surface to the exit surface. Figure 7 shows that as the plate cools, the oxygen concentration increases until it reaches the uniform ambient condition.

TABLE 2 --- Geometry of porous medium and ambient conditions for the example problems in Section 2.4.1

| | |
|---|---|
| Particle Shape: | spherical |
| Particle Diameter ( $d$ ): | .005 in |
| Unit Cell Thickness ( $D$ ): | .005 in |
| Spatial Thickness of Porous Medium ( $L$ ): | .25 in |
| Porosity ( $p$ ) | .476 |
| Permeability ( $m$ ) | $.162 \times 10^{-9}$ $ft^2$ |
| Bulk Thermal Conductivity of Carbon ( $k_c$ ): | 86.0 Btu/ft-hr-F |
| Bulk Specific Heat of Carbon ( $c_c$ ): | .231 Btu/lbm-F |
| Bulk Density of Carbon ( $\rho_c$ ): | 70.3 $lbm/ft^3$ |
| Thermal Emissivity of Particles ( $\epsilon$ ): | .9 |
| Ambient Temperature ( $T_\infty$ ): | 80.0 deg-F |
| Ambient Pressure ( $P_\infty$ ): | 14.7 psi |
| Pressure Differential ( $\Delta P$ ): | -.35 psi |
| Ambient Oxygen Concentration ( $\phi_{1\infty}$ ): | .0172 $lbm/ft^3$ |

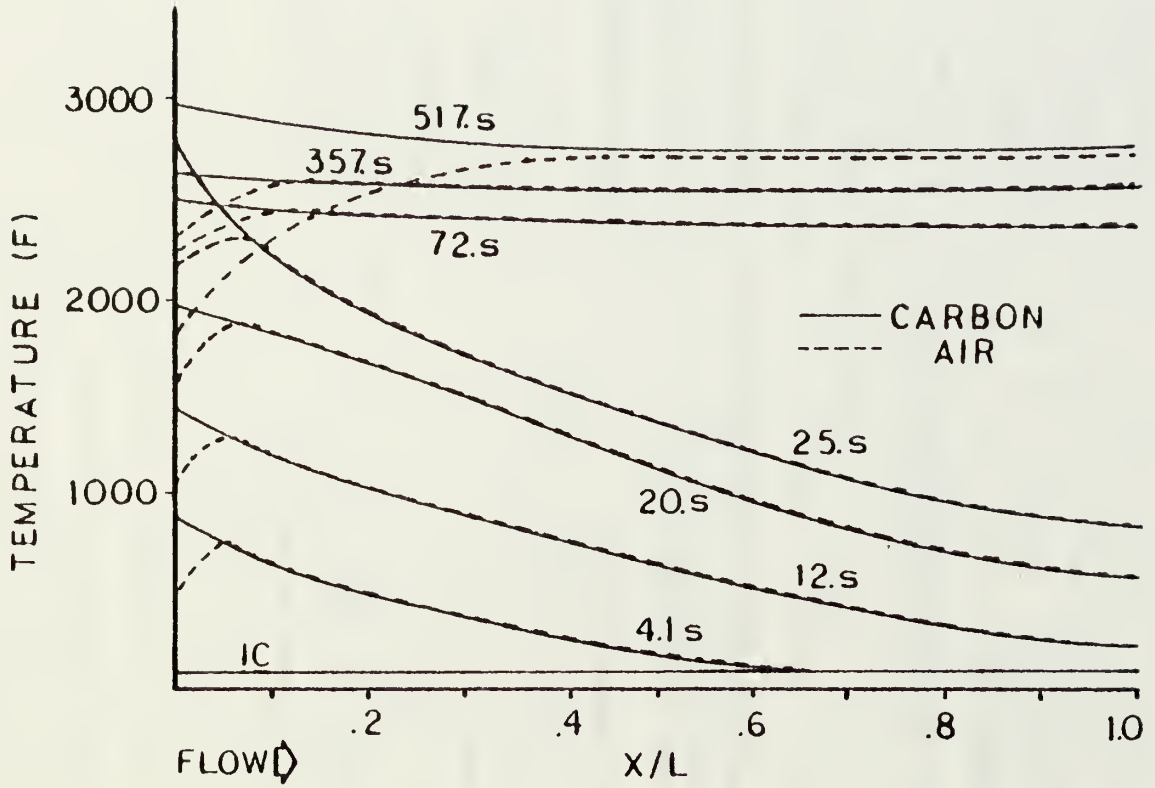


FIGURE 3 --- Sustained combustion resulting from a heat flux at the x = 0 surface.

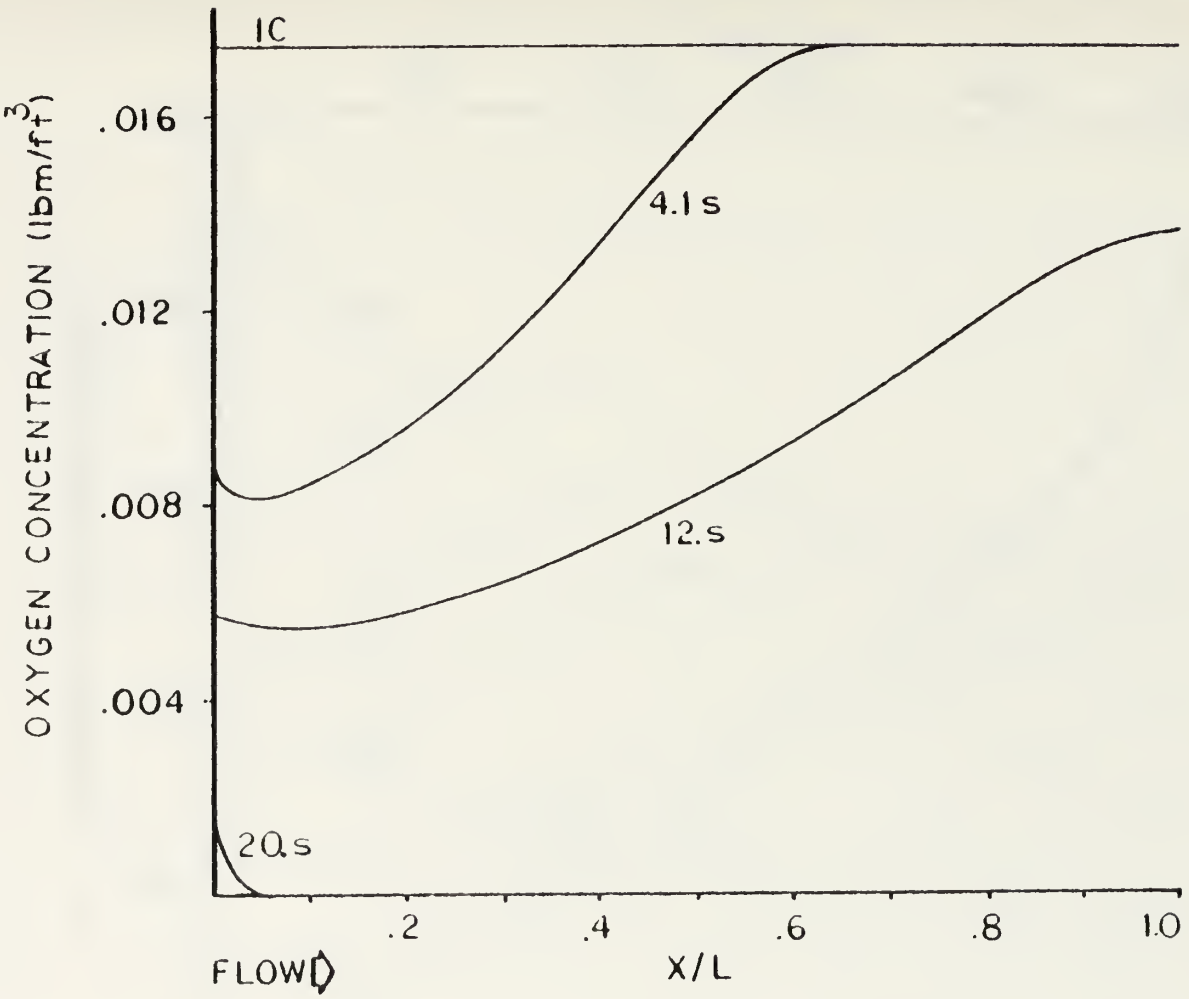


FIGURE 4 --- Oxygen response during sustained combustion.

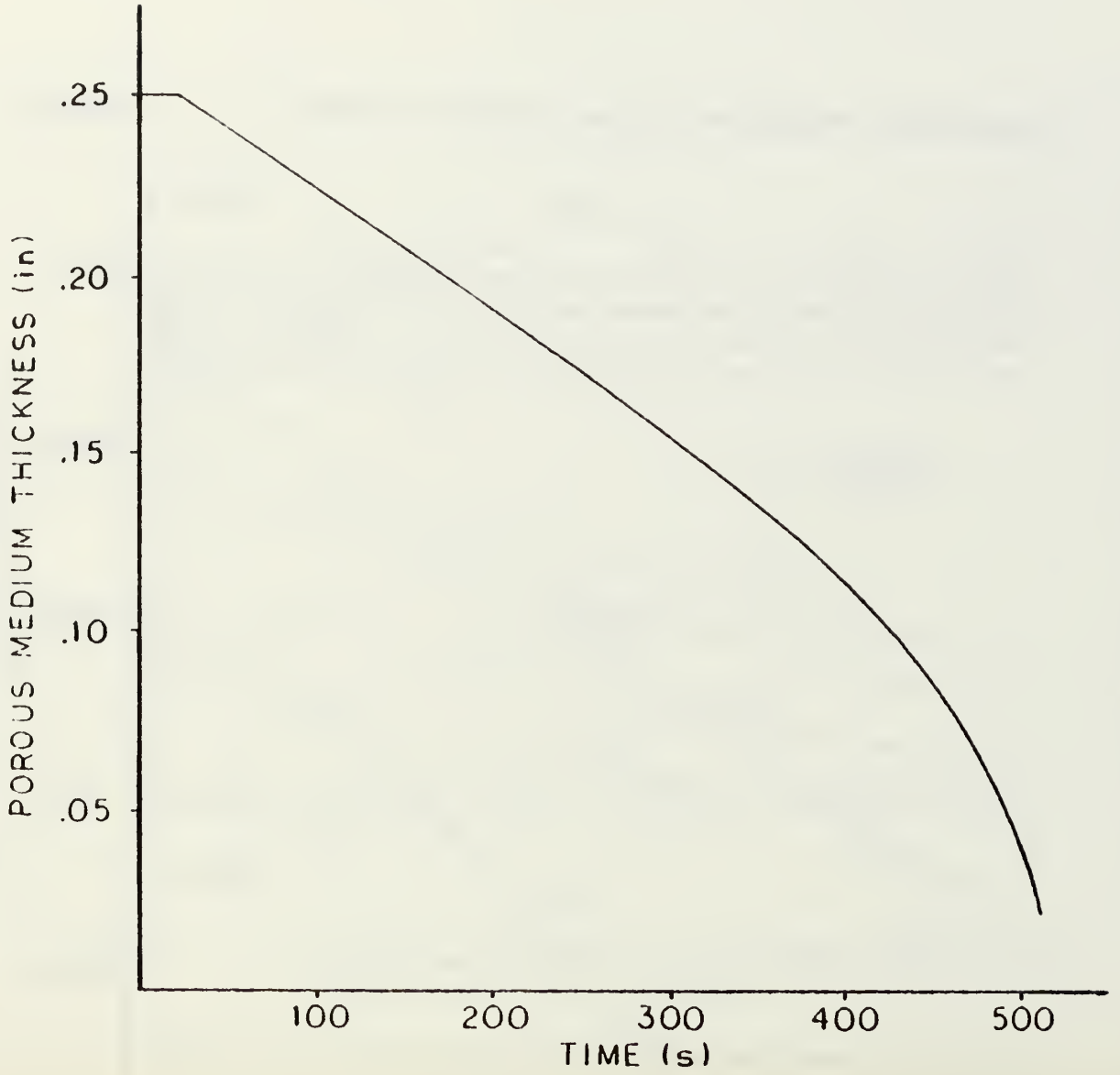


FIGURE 5 --- Change in thickness of porous medium during surface recession phase.

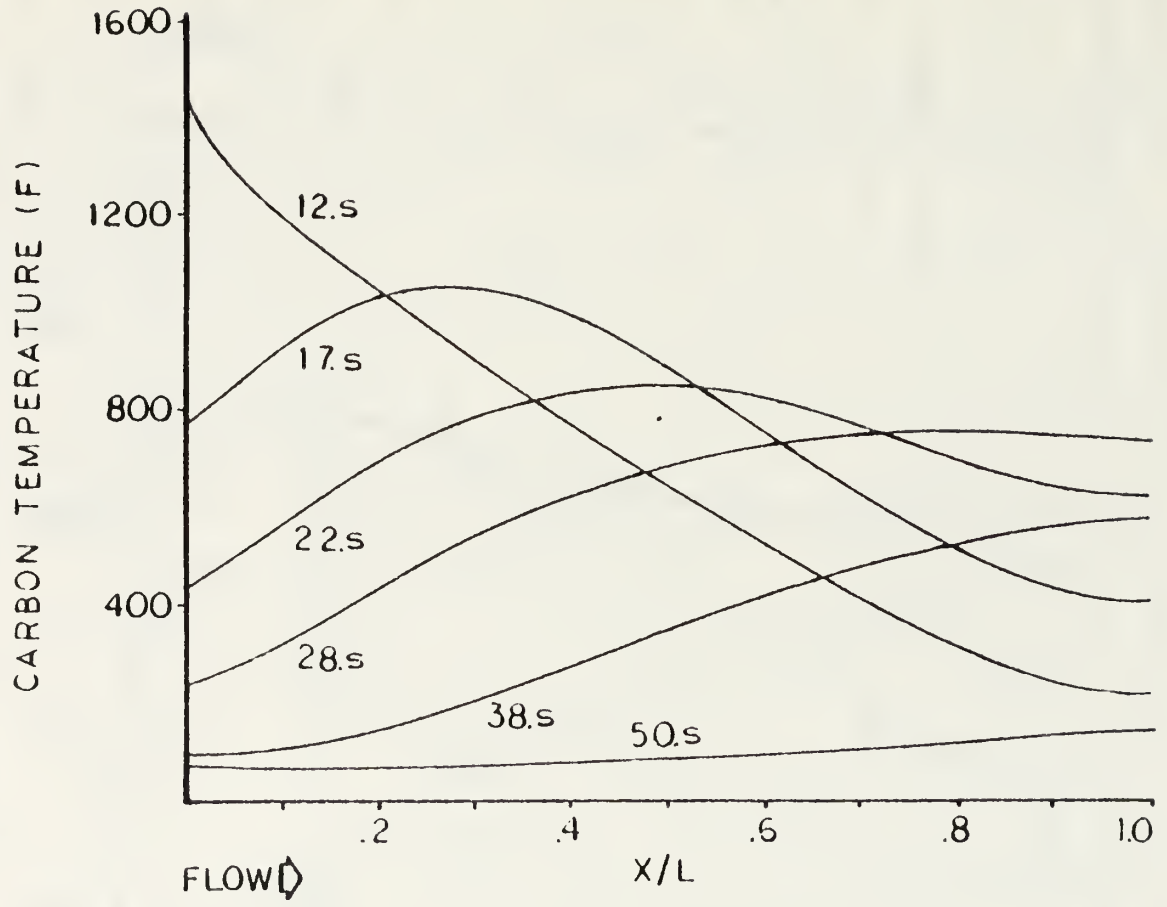


FIGURE 6 --- Response of temperature when heat flux at x = 0 insufficient to produce sustained combustion.

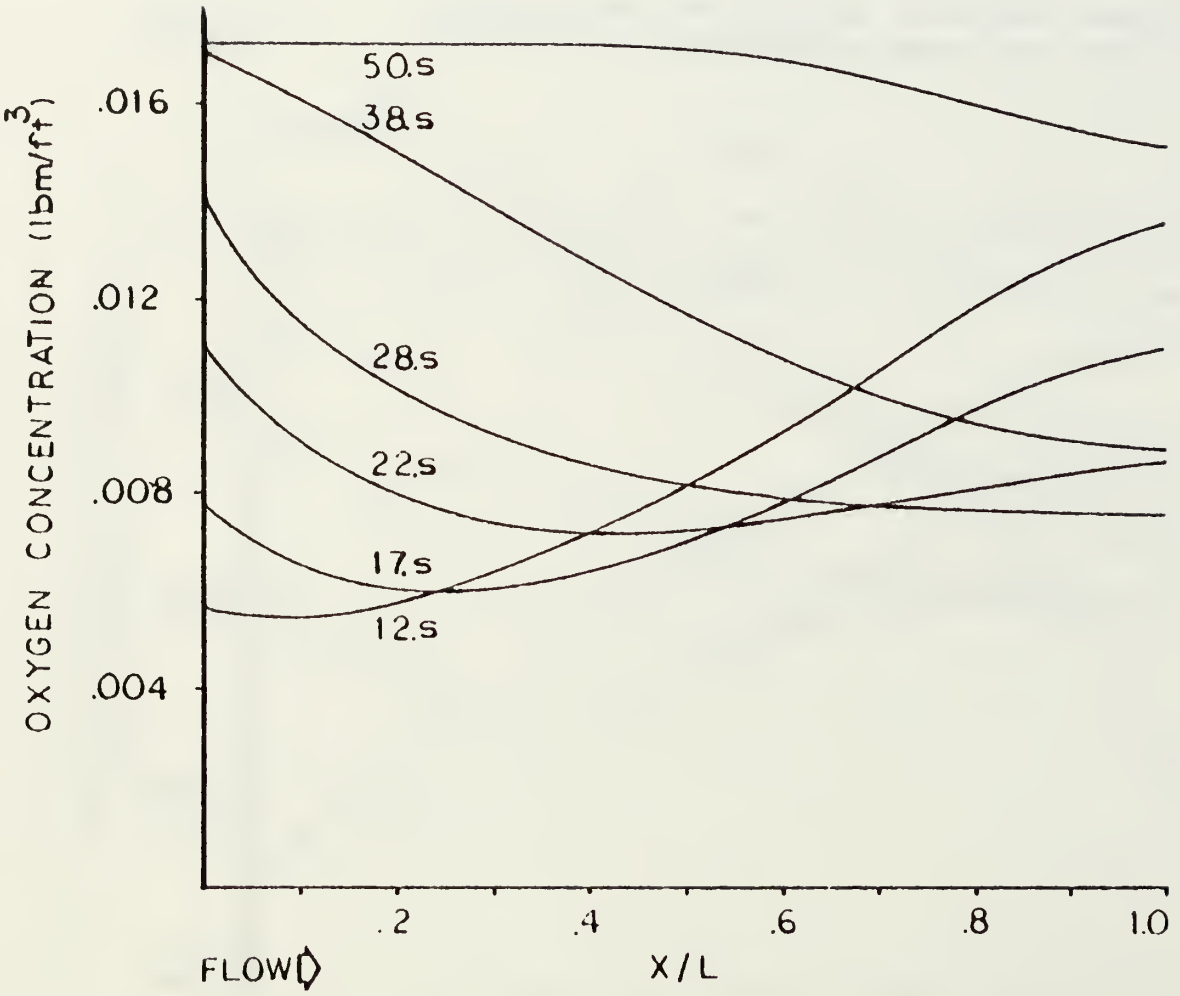


FIGURE 7 --- Response of oxygen as porous medium cools to ambient temperature.

The point to be made here is that a slight change in the duration of heat flux can determine whether damaging combustion or safe extinction occurs. Here we have seen that 30,000 Btu/ft-hr for 15 seconds results in a combustion which completely consumed the plate. The same plate goes to extinction if the heat flux is terminated after 14 seconds.

### 2.4.2 Effects of Permeability

Permeability, a measure of flow conductance, is one of the composite design parameters which most affects thermal behavior. In order to isolate the effect of permeability on behavior, the geometry of the filament diameter and the width of the unit cell were varied in such a way as to maintain a constant porosity for all analyses in this study. In this way, the quantity of air around a filament at any instant is fixed, but the rate of air passing a filament increases with increasing permeability. Table 3 lists the data for a number of analyses which were used in the permeability study. Figure 8 presents temperature versus permeability for three values of pressure differential. The temperature here is the temperature above which the plate will experience combustion, and below which the plate will extinguish. The "ignition" temperature for each case is obtained by trial and error iteration on a uniform initial temperature. After a number of runs, we obtain two nearly equal uniform initial temperatures, one leading to combustion and the other extinguishment. Their average is taken as the "ignition" temperature.

Figure 8 shows that for a given permeability, the temperature at which combustion occurs increases with increasing pressure differential. An increase in the pressure differential causes an increase in the air flow through the porous medium. Here an increase in air flow results in "blowout" extinguishment. That is, an increase in air flow results in an increase in the ignition temperature. We also note that the rate of change of ignition temperature decreases with increasing permeability.

TABLE 3 --- Geometry of porous medium and ambient conditions for the permeability analysis in Section 2.4.2

| | |
|---|---|
| Particle Shape: | spherical |
| Particle Diameter ($d$): | (various) |
| Unit Cell Thickness ($D$): | (various) |
| Spatial Thickness of Porous Medium ($L$): | 1.0 in |
| Porosity ($p$) | .476 |
| Permeability ($m$) | (various) |
| Bulk Thermal Conductivity of Carbon ($k_c$): | 86.0 Btu/ft-hr-F |
| Bulk Specific Heat of Carbon ($c_c$): | .231 Btu/lbm-F |
| Bulk Density of Carbon ($\rho_c$): | 70.3 lbm/ft$^3$ |
| Thermal Emissivity of Particles ($\epsilon$): | .9 |
| Ambient Temperature ($T_\infty$): | 80.0 deg-F |
| Ambient Pressure ($P_\infty$): | 14.7 psi |
| Pressure Differential ($\Delta P$): | (various) |
| Ambient Oxygen Concentration ($\phi_\infty$): | .0172 lbm/ft$^3$ |

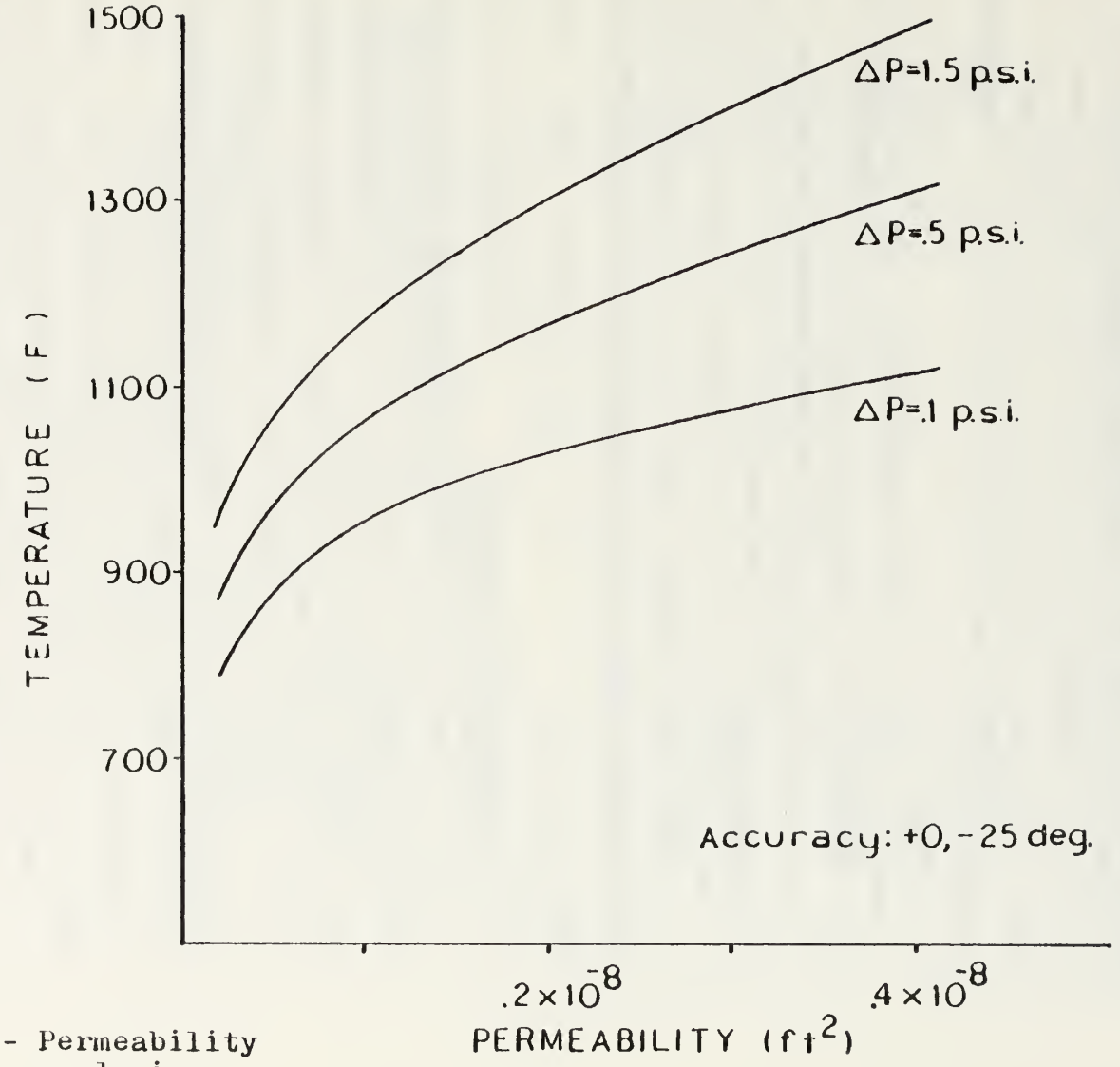


FIGURE 8 --- Permeability analysis.

### 2.4.3 Effects of Porosity

The affect of porosity, the measure of void volume per unit volume of space, on thermal behavior is shown in Figure 9. The data for the porosity study is given in Table 4. Figure 9 shows that for a fixed porosity, the ignition temperature increases with increasing permeability. Again this shows that increasing the air flow will cause blowout at a fixed temperature, or stating it a little differently, increasing the air flow through a plate makes it less likely to combust.

However, given a fixed permeability, the ignition temperature decreases with increasing porosity. The reason for this is that increasing the porosity while fixing all other parameters results in decreasing air flow through the medium. We note that the rate of change of ignition temperature diminishes with porosity. That is, the decrease of ignition temperature with porosity becomes less with increasing porosity.

### 2.4.4 Effects of Thickness

Figure 10 shows the effect of plate thickness on thermal behavior. Table 5 is the data for the thickness study. The most important feature of Figure 10 is the very large decrease in ignition temperature with thickness, especially for the smaller thicknesses from 0.25 inches to 2.0 inches. An explaination for this behavior is the following. If all parameters except thickness are fixed, then increasing the thickness while keeping the pressure differential constant results in decreasing the pressure gradient. The decrease in pressure gradient causes a decrease in the pore velocity of the air through the plate. Thus, increasing thickness results in a decrease of air flow. With less air flow, convective heat transfer diminishes and there is less opportunity for blowout. Hence an increase in thickness should result in a lower ignition temperature.

Another explaination for decreasing ignition temperature with increasing thickness is as follows. The above sentence

TABLE 4 --- Geometry of porous medium and ambient conditions for the porosity analysis in Section 2.4.3

| | |
|---|---|
| Particle Shape: | spherical |
| Particle Diameter ( $d$ ): | (various) |
| Unit Cell Thickness ( $D$ ): | (various) |
| Spatial Thickness of Porous Medium ( $L$ ): | 1.0 in |
| Porosity ( $p$ ) | (various) |
| Permeability ( $m$ ) | (various) |
| Bulk Thermal Conductivity of Carbon ( $k_c$ ): | 86.0 Btu/ft-hr-F |
| Bulk Specific Heat of Carbon ( $C_c$ ): | .231 Btu/lbm-F |
| Bulk Density of Carbon ( $\rho_c$ ): | 70.3 $lbm/ft^3$ |
| Thermal Emissivity of Particles ( $\epsilon$ ): | .9 |
| Ambient Temperature ( $T_\infty$ ): | 80.0 deg-F |
| Ambient Pressure ( $P_\infty$ ): | 14.7 psi |
| Pressure Differential ( $\Delta P$ ): | -.5 psi |
| Ambient Oxygen Concentration ( $\phi_\infty$ ): | .0172 $lbm/ft^3$ |

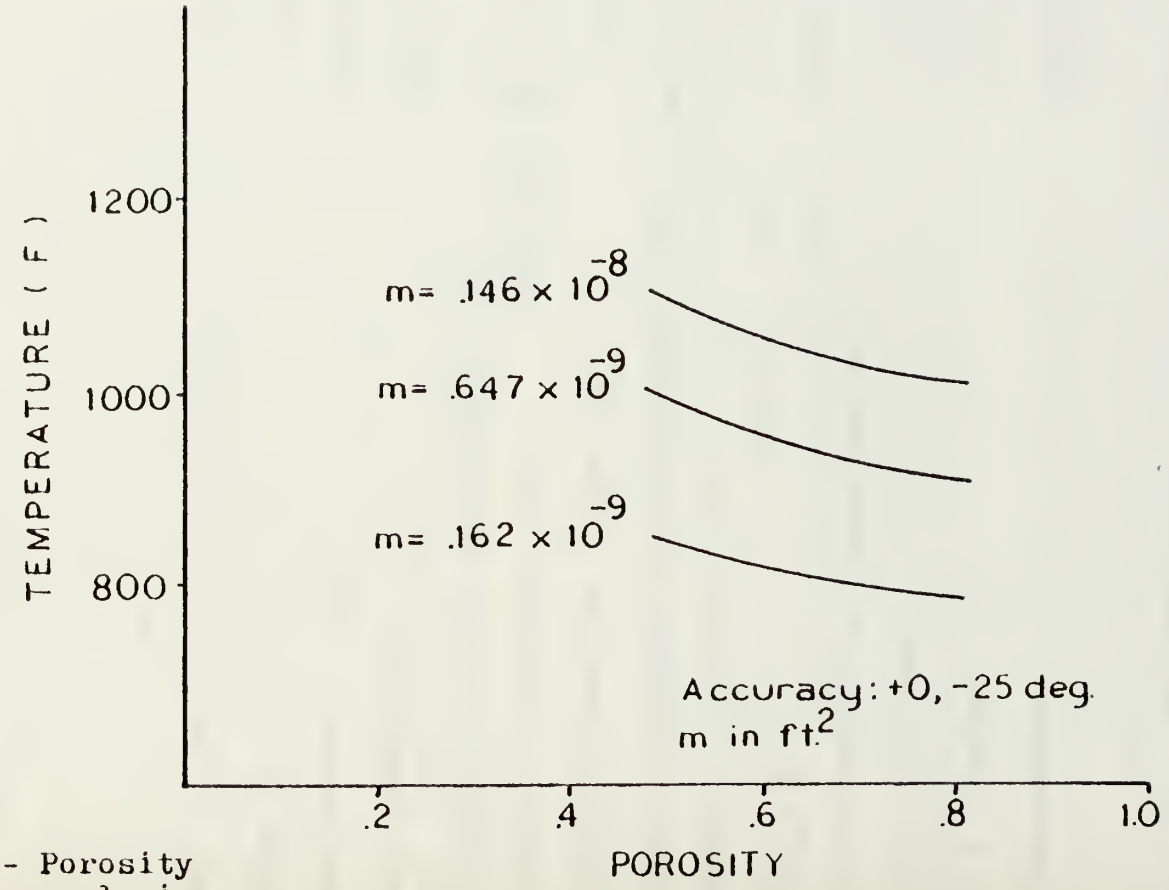


FIGURE 9 --- Porosity analysis.

TABLE 5 --- Geometry of porous medium and ambient conditions for the thickness analysis in Section 2.4.4

| | |
|---|---|
| Particle Shape: | spherical |
| Particle Diameter ( $d$ ): | (various) |
| Unit Cell Thickness ( $D$ ): | (various) |
| Spatial Thickness of Porous Medium ( $L$ ): | (various) |
| Porosity ( $\rho$ ) | .476 |
| Permeability ( $m$ ) | (various) |
| Bulk Thermal Conductivity of Carbon ( $k_c$ ): | 86.0 Btu/ft-hr-F |
| Bulk Specific Heat of Carbon ( $c_c$ ): | .231 Btu/lbm-F |
| Bulk Density of Carbon ( $\rho_c$ ): | 70.3 $lbm/ft^3$ |
| Thermal Emissivity of Particles ( $\epsilon$ ): | .9 |
| Ambient Temperature ( $T_\infty$ ): | 80.0 deg-F |
| Ambient Pressure ( $P_\infty$ ): | 14.7 psi |
| Pressure Differential ( $\Delta P$ ): | -.5 psi |
| Ambient Oxygen Concentration ( $\phi_\infty$ ): | .0172 $lbm/ft^3$ |

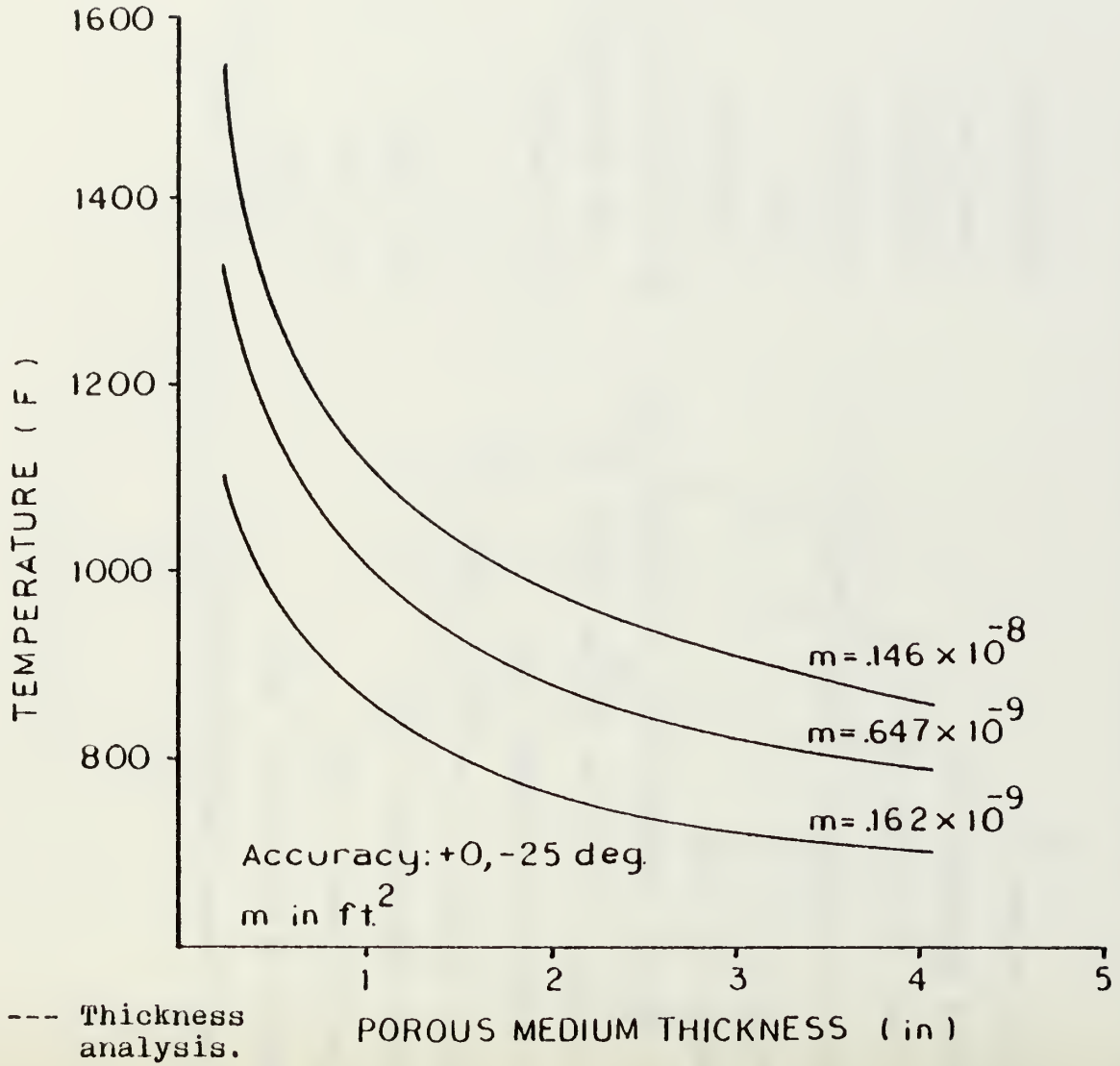


FIGURE 10 --- Thickness analysis.

can be turned around to "decreasing the thickness will result in increasing the ignition temperature". Now the thinner the plate, the less distance the air traverses in passing through the plate. Since the air temperature increases as it passes through the plate, thin plates have a larger fraction of their region with cool air than do thick plates. As thin plates are more effectively cooled by the air flow, higher ignition temperatures are needed for combustion.

The three curves again show that increasing the pore velocity by increasing the permeability, leads to blowout, and hence greater air flow (or, equivalently, permeability) leads to higher ignition temperatures.

Another striking feature of Figure 10 is the rapid decrease in the rate of change of ignition temperature with thickness. A large change in the ignition temperature can be effected by a small change in the thickness when the plate is thin. On the other hand, very little change in the ignition temperature can be effected if the plate is very thick.

### 2.4.5 Effects of Pressure Differential

Each of the previous studies sought to determine the effect of a design parameter on system behavior. These parameters are, generally, under the control of the structural engineer, and thus can be selected to minimize combustion. In contrast, there are external parameters such as pressure differential (possibly arising from wind over one surface) which are difficult, if at all possible, to control.

Table 6 presents the data for the pressure differential study, and Figure 11 presents the results of the study. The results show that the ignition temperature increases with increasing pressure differential, and that the rate of increase decreases with pressure differential. As in the previous studies, it is again evident that an increase in permeability results in higher ignition temperatures. The three curves in Figure 11 show that the effect of pressure differential is much greater for larger values of permeability.

### 2.4.6 Effects of Boundary Conditions

All of the the previous parameter studies were performed using insulated boundary conditions at the inlet and exit surfaces. In this study, the effect of heat transfer at the boundaries was investigated. Figure 12 compares the behavior of plates with insulated boundaries (curve B) to plates with heat transfer at the boundaries (curve A). Although the ignition temperatures for the plates with heat transfer are always greater than the ignition temperatures for the insulated plates, two regions are distinguishable. In the region with permeability greater than 0.2x10-8 in. , the ignition temperatures for insulated plates are but slightly less than for the heat transfer plates. In the region with permeability less than 0.2x10-8 in. , there is a far more pronounced difference between insulated plates and plates with heat transfer. The results show that as permeability decreases, the ignition temperature decreases in both cases, but the rate of decrease is larger for the insulated case, and thus the difference between ignition temperatures becomes increasingly greater. Finally, at some small value of permeability, the ignition temperature for plates with surface heat transfer reverses and begins increasing rapidly with decreasing permeability.

An increase in the ignition temperature with decreasing air flow (permeability) for plates with heat transfer boundary conditions could be explained if the heat generation by the exothermal reaction , and not the heat transfer mechanism, was the dominating mechanism. In this case the reduction of oxygen resulting from a decrease in permeability would extinguish the combustion by "choking". In the choking region, ignition temperatures should increase with decreasing permeability.

Apparently, porous plates with heat transfer boundary conditions have a minimum ignition temperature at a particular value of air flow, say U. Increasing the air flow above U results in combustion extinguishment by blowout and hence greater ignition temperatures. This is the case when heat

TABLE 6 --- Geometry of porous medium and ambient conditions for the pressure differential analysis in Section 2.4.5

| | |
|---|---|
| Particle Shape: | spherical |
| Particle Diameter ( $d$ ): | (various) |
| Unit Cell Thickness ( $D$ ): | (various) |
| Spatial Thickness of Porous Medium ( $L$ ): | 1.0 in |
| Porosity ( $p$ ) | .476 |
| Permeability ( $m$ ) | (various) |
| Bulk Thermal Conductivity of Carbon ( $k_c$ ): | 86.0 Btu/ft-hr-F |
| Bulk Specific Heat of Carbon ( $C_c$ ): | .231 Btu/lbm-F |
| Bulk Density of Carbon ( $\rho_c$ ): | 70.3 $lbm/ft^3$ |
| Thermal Emissivity of Particles ( $\epsilon$ ): | .9 |
| Ambient Temperature ( $T_\infty$ ): | 80.0 deg-F |
| Ambient Pressure ( $P_\infty$ ): | 14.7 psi |
| Pressure Differential ( $\Delta P$ ): | (various) |
| Ambient Oxygen Concentration ( $\phi_{1\infty}$ ): | .0172 $lbm/ft^3$ |

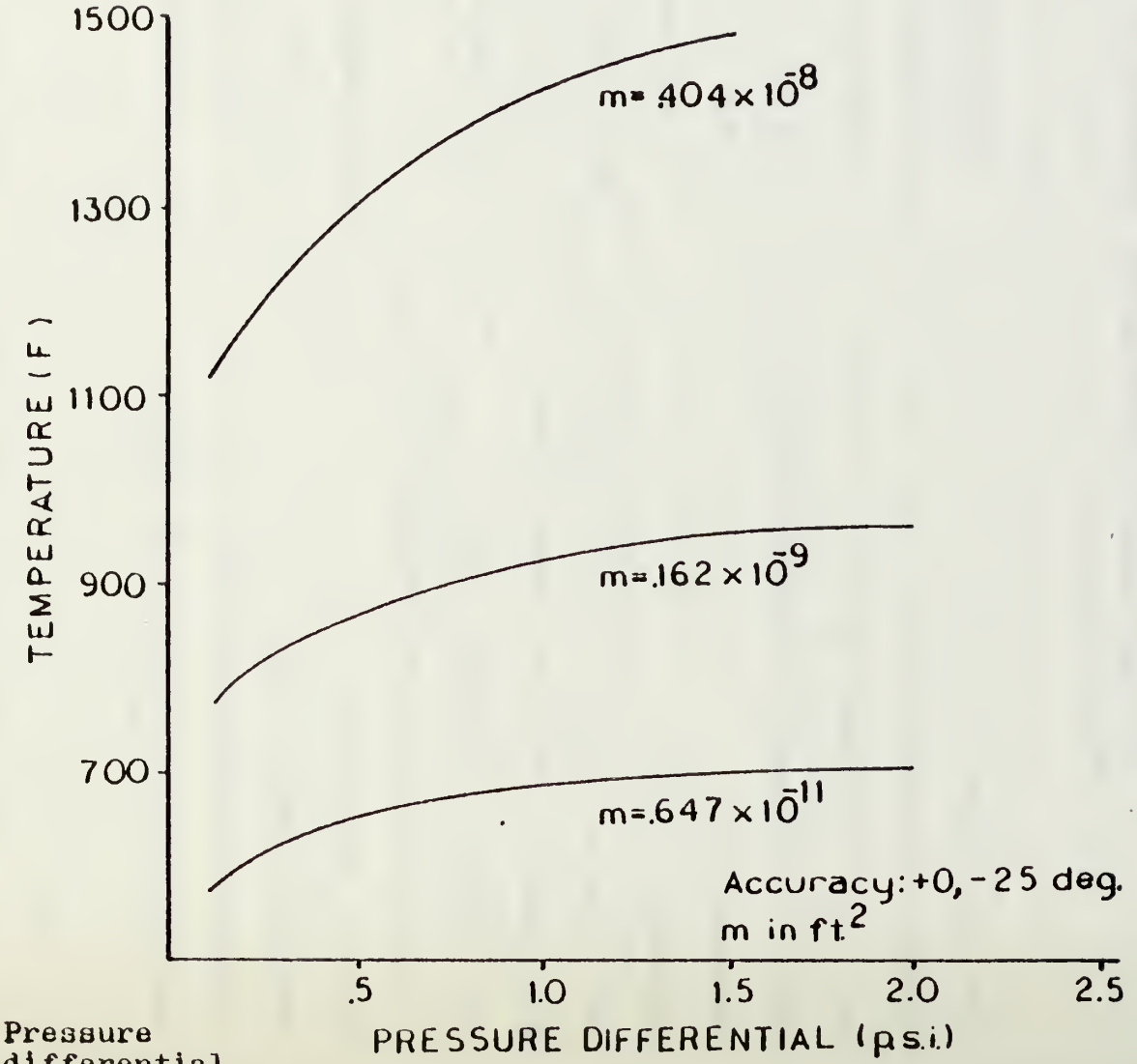


FIGURE 11 --- Pressure differential analysis .

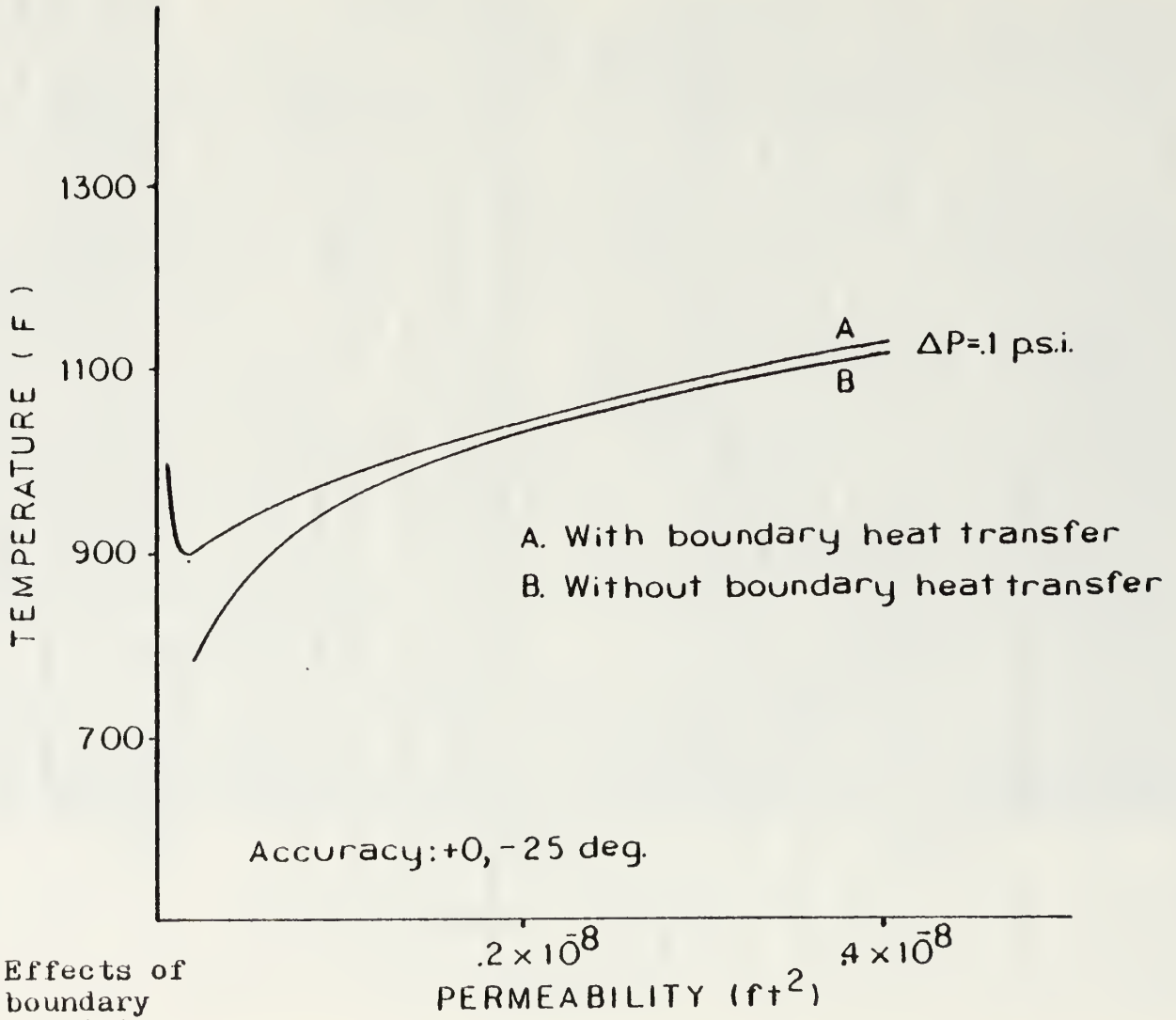


FIGURE 12 --- Effects of boundary conditions.

transfer is the dominant mechanism. On the other hand, decreasing the air flow below U results in combustion extinguishment by choking and hence greater ignition temperatures. This is the case when the chemical reaction is the dominant mechanism.

### 2.4.7 Effects of Pore Velocity

Consideration of the results of the previous studies on the effects of individual parameters on system behavior suggests that the most important parameter affecting behavior is the pore velocity. With this in mind, the results of all computer analyses (47 problems) are shown in Figure 13. The curve through these data points is a fair fit, and thus there is reason to believe that the ignition temperature may be obtained, with fair accuracy, by the equation of the curve.

This concludes the summary of the work done by Lcdr. Vatikiotis at NSRDC for his Doctor of Engineering Degree. The dissertation, a more general treatment of the combustion problem, presents a more detailed discussion of the model, numerical aspects of the formulation, the results, and conclusions. In addition, there is a discussion of a generalized Semenov model for combustion of porous media, as well as an extensive list of references.

## 2.5 NPS ACTIVITY

During the past year, about half of the funded research activity at NPS was devoted to the thermal investigation, and the other half was given to the strength investigation. In this section, a summary of the effort of the thermal investigation at NPS will be described.

### 2.5.1 Restart Capability

One of the input parameters in the thermal analysis program (CARBGT) is the time that the user would like the analysis to stop. It is difficult to select a reasonable value for this parameter. Selecting too large a time is wasteful

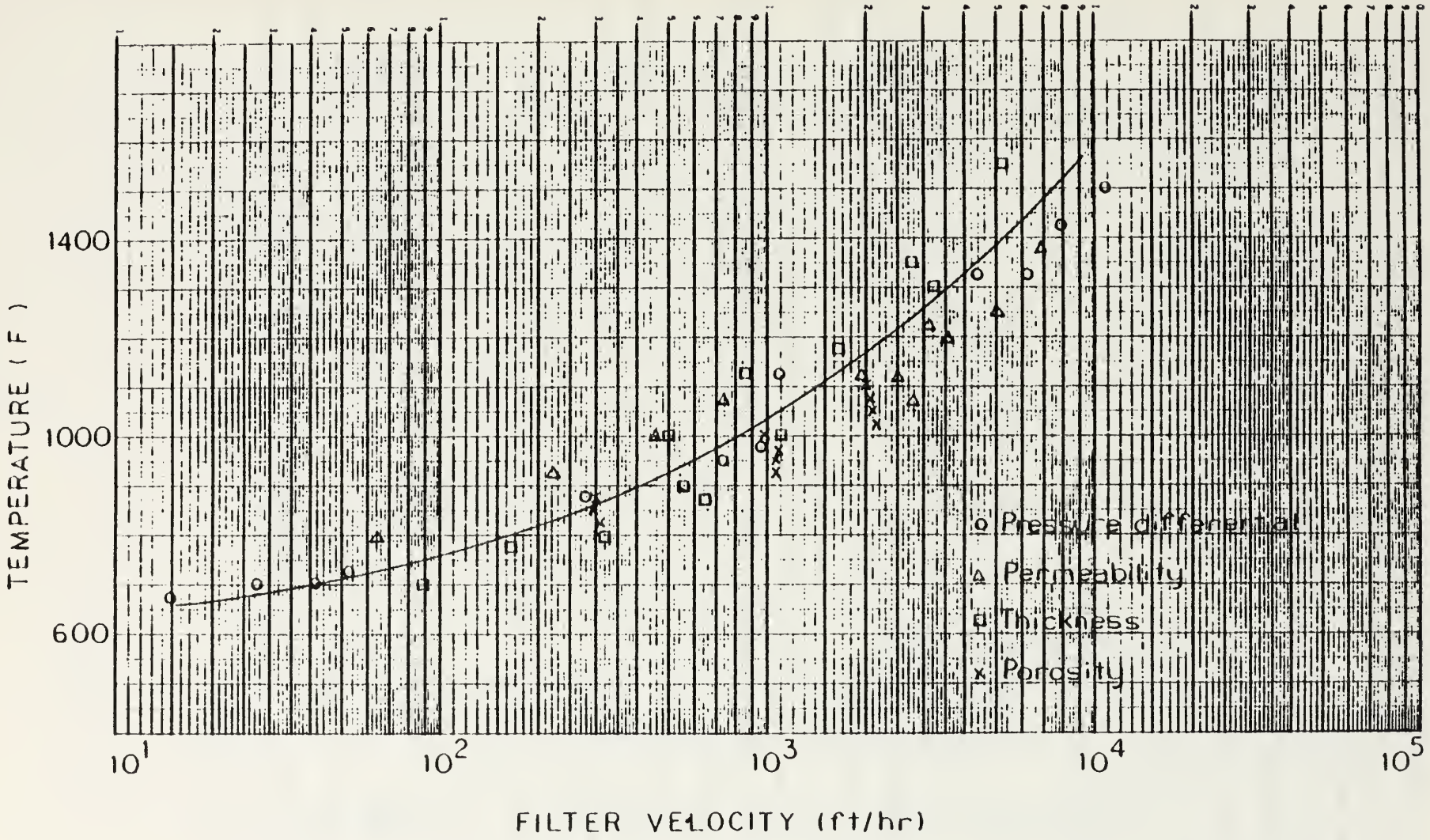


FIGURE 13 --- "Minimum initial temperature" as a function of pore velocity.

of computer effort, while too small a time could require redoing the problem. To remedy this situation, a subroutine was added to the program to permit restart. The restart feature permits the program to start from the results of a previous analysis. All of the input data necessary for the restart analysis is obtained from the final output of the previous analysis. Restart can be invoked in the analysis of a problem as many times as desirable. In this way, a complete analysis of a problem may consist of several time contiguous analyses.

### 2.5.2 Effects of Initial Conditions

There are two ways to input initial conditions. A way to obtain reasonable initial conditions on temperature is to specify a heat flux and a duration time, as described in section 2.3.9. On the other hand, if the user is interested in the effects of the initial temperature on thermal behavior, he may input any initial temperature distribution. This was the method used in this investigation. Here we obtained the effects of linear initial temperature distributions on ignition temperature in the following way. The slope of the linear temperature and the average temperature was specified. The same problem was run as many times as needed to obtain the average temperature below which extinction occurs and above which combustion occurs. Figure 14 presents the results of this study. Two features of this figure are (1) the maximum ignition temperature occurs for a negative temperature slope, and (2) the ignition temperatures are greater for the negative temperature slopes. Figure 14 shows that combustion is less likely to occur for plates with the higher temperature on the X/L=0. surface. This is a reasonable expectation since the cooling air is most effective at it's entry into the medium.

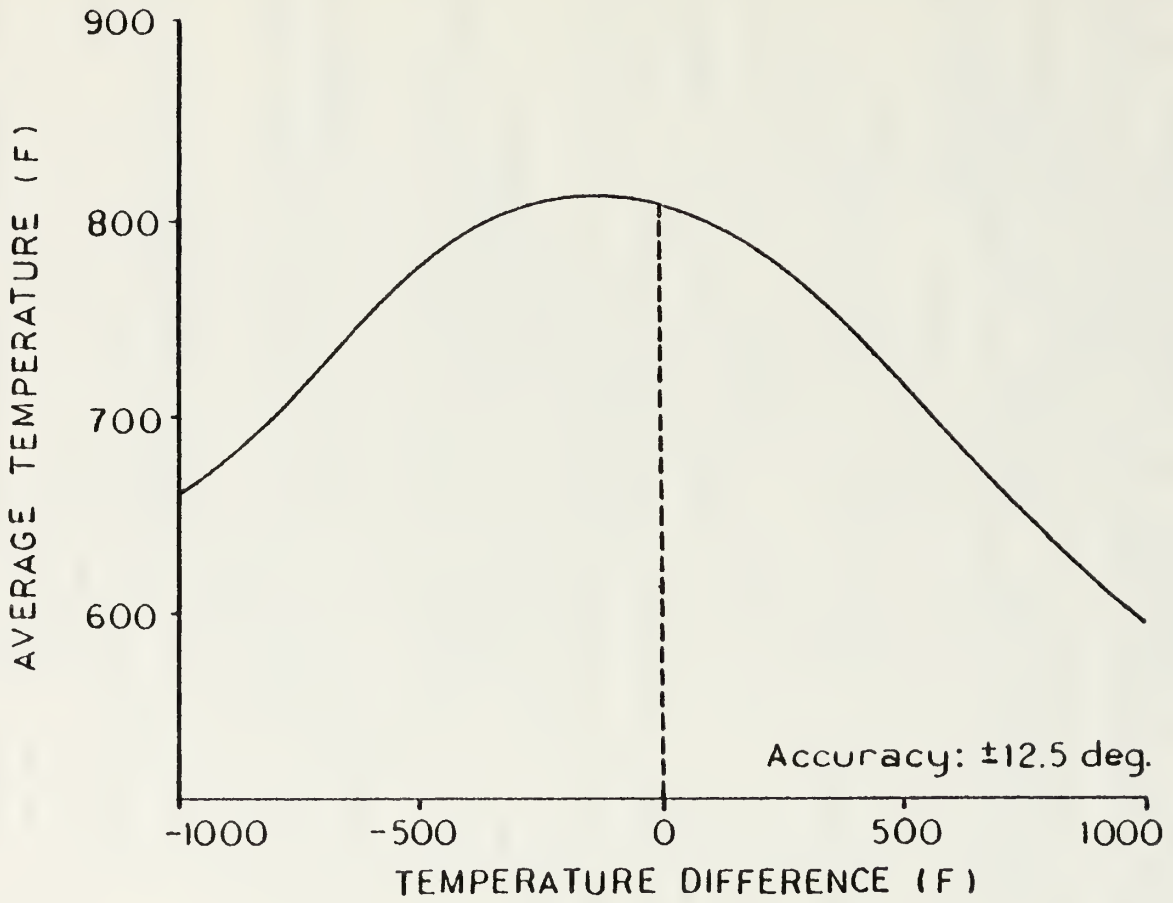


FIGURE 14 --- Results of initial condition analysis.

### 2.5.3 Graphics Capability

Each computer analysis produces a vast quantity of numerical output. Thus, at preselected instances of time and at each spatial nodal point, the program reports: (a) graphite temperature, (b) air temperature, (c) oxygen concentration, (d) reaction rate, (e) filament diameter (f) porosity, (g) permeability, (h) pressure, (i) pressure gradient (j) pore velocity (k) Reynolds Number, (l) convection coefficient, and (m) area to volume ratio. In addition, plate thickness is reported at each time. This data must be assimilated by the program user if full benefit of the analysis is to be obtained. As a typical analysis consists of 30 to 60 time steps and 25 to 40 spatial nodal points, a typical output contains anywhere from 10,000 to 30,000 numbers. It is difficult, if at all possible, to assimilate this quantity of numerical data, and therefore graphical output is more than just desirable, it is necessary. To this end, graphics capability was incorporated into the program. A variety of graphics options are now available. The user may select any combination of the following output modes:

1. numerical results of all system parameters,
2. curves of graphite temperature and oxygen concentration as functions of space at preselected time instances,
3. three dimensional surfaces of graphite temperature, oxygen concentration, and reaction rate as functions of time and space,
4. contour graphs of graphite temperature, oxygen concentration, and reaction rate.

Any combination of these options is available at a CRT terminal or as hard copy output.

Two programs exist for the surface and contour graphics. GRAF3D produces surfaces and/or contours from the actual numerical output of the analysis program, while GRAF3E achieves smoother graphics by passing the output from CARBGT through a cubic spline interpolation subroutine (IMSL subroutine IBCIEU).

After inspecting the graphical output from GRAF3D or GRAF3E, it may be desirable to have a more detailed surface or contour of a local subregion of the time-space domain. This may be done by recalling either graphics program, and specifying the upper and lower limits of the time and space subregion of interest. Figures 15 through 20 are sample output of surfaces and contours from GRAF3D. Figures 21 through 26 , are samples of subregion graphics of the same analysis as Figures 15 through 20.

This concludes the discussion of the research on the thermal investigation. A description of the strength investigation follows.

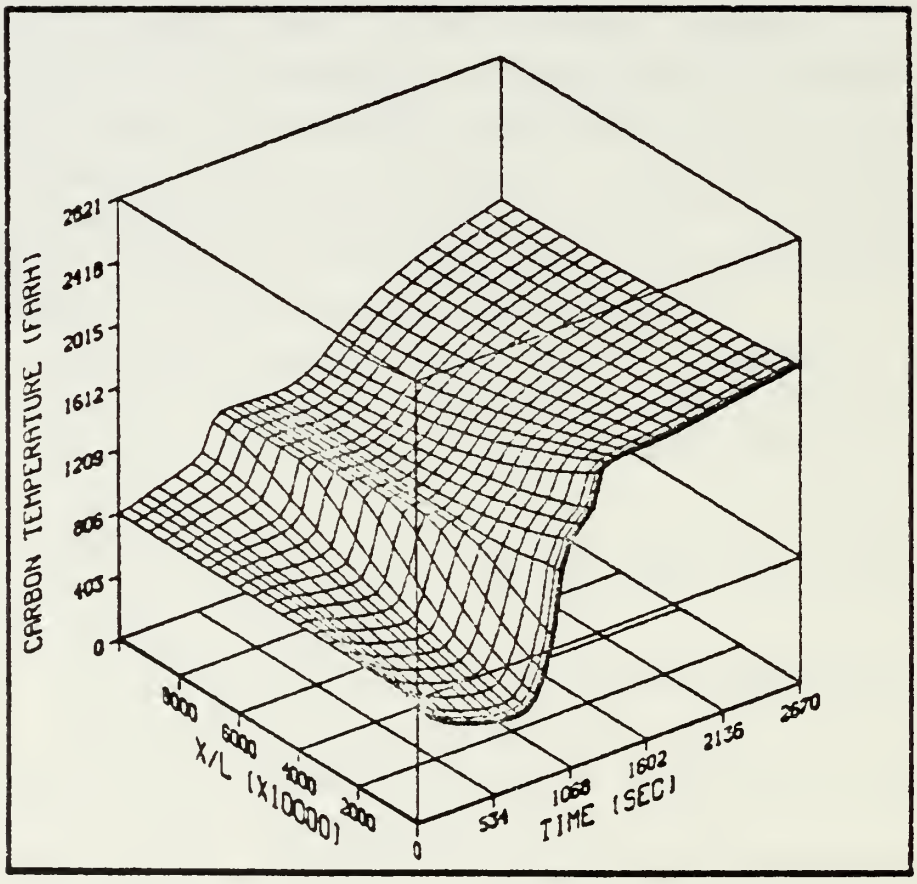


Figure 15. Temperature Surface from GRAF3D

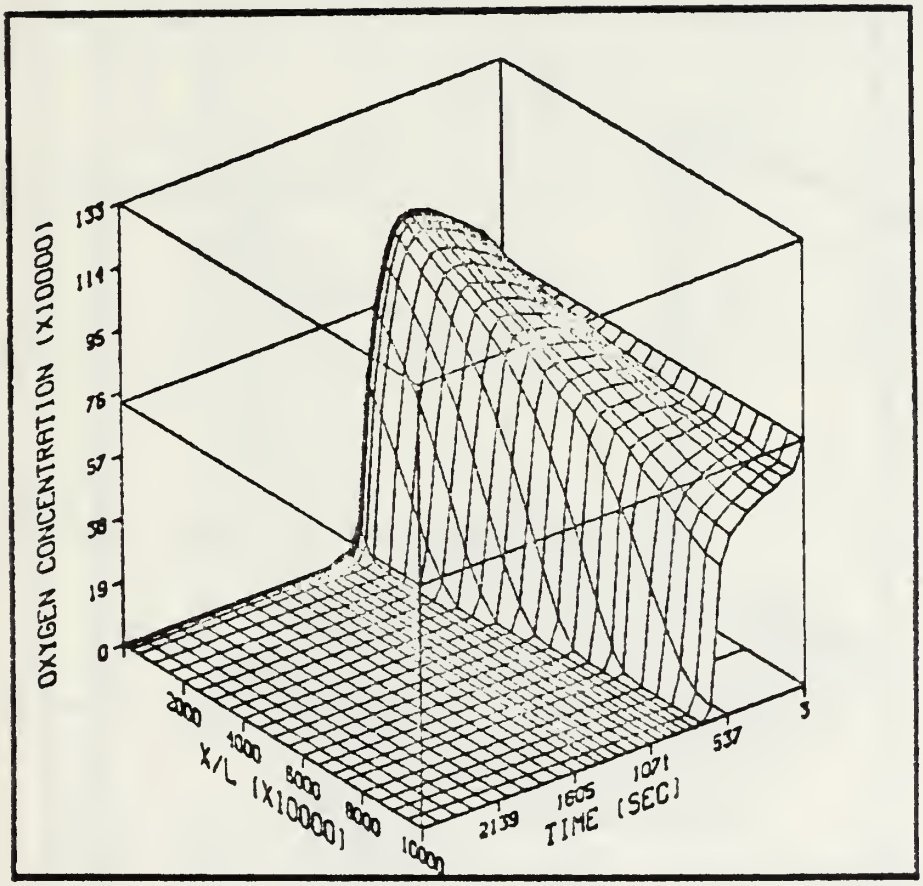


Figure 16. Concentration Surface from GRAF3D

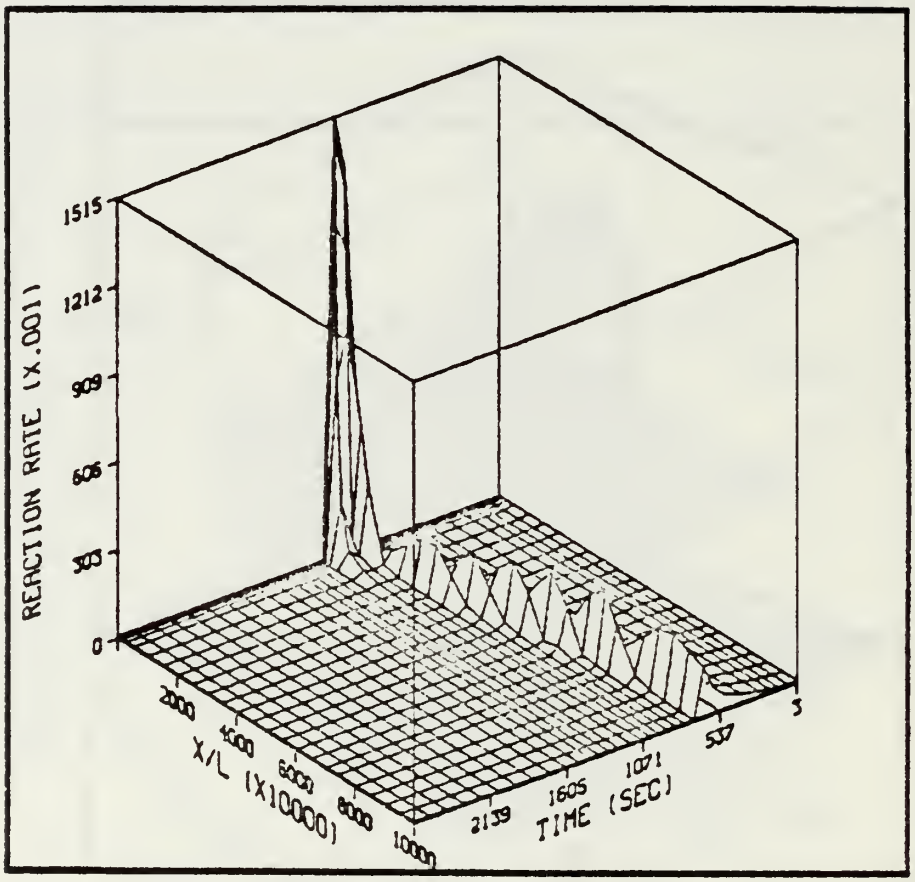


Figure 17. Reaction Rate Surface from GRAF3D

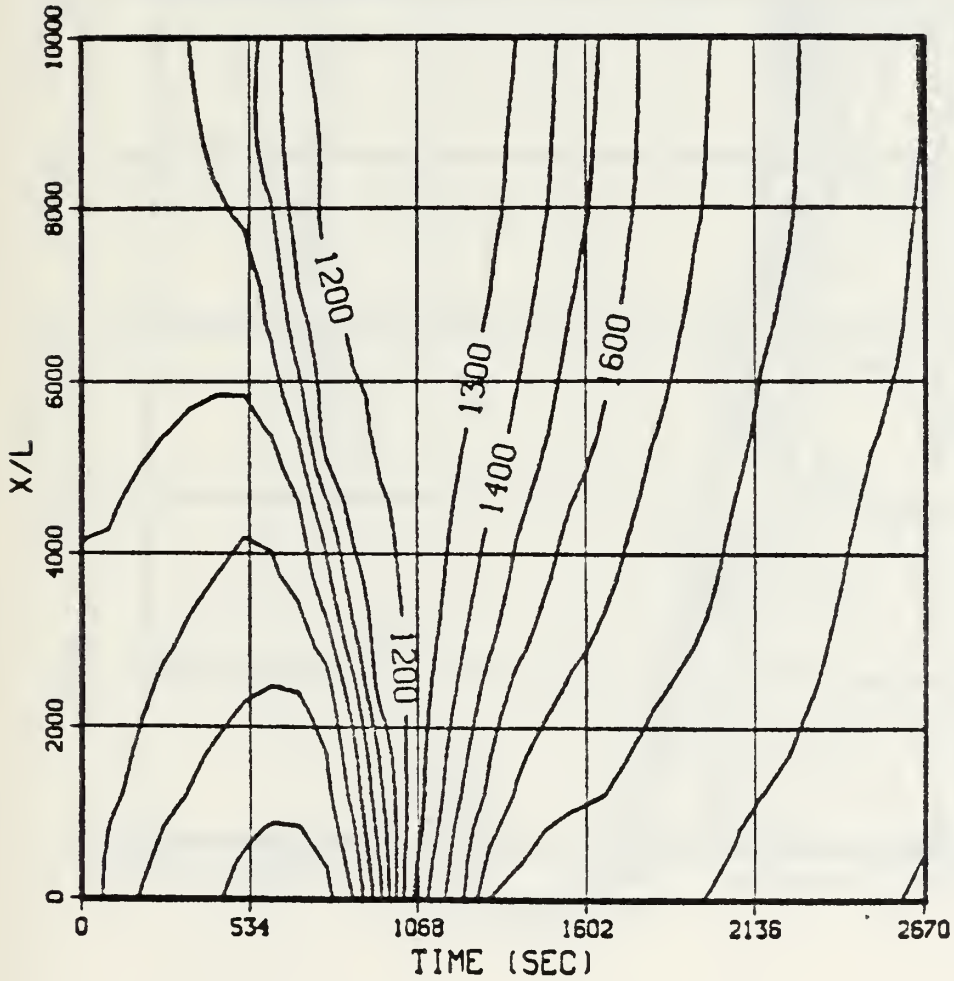


Figure 18. Temperature Contours from GRAF3D

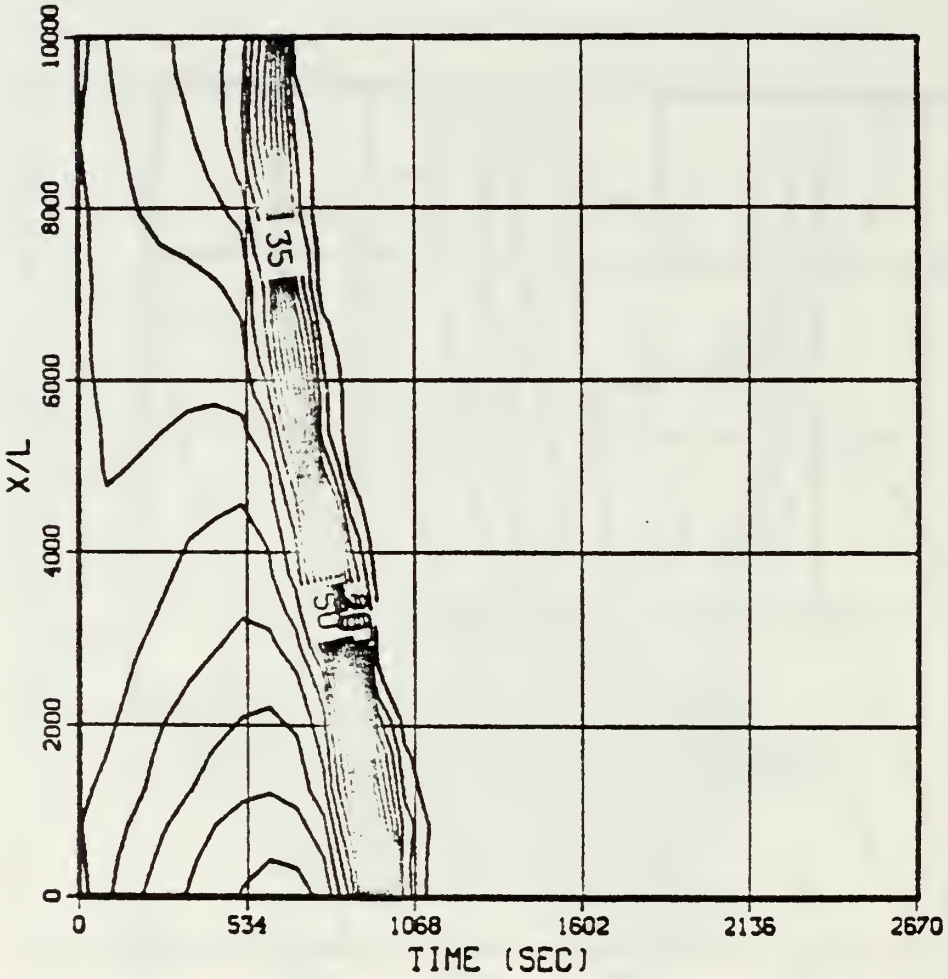


Figure 19. Concentration Contours from GRAF3D

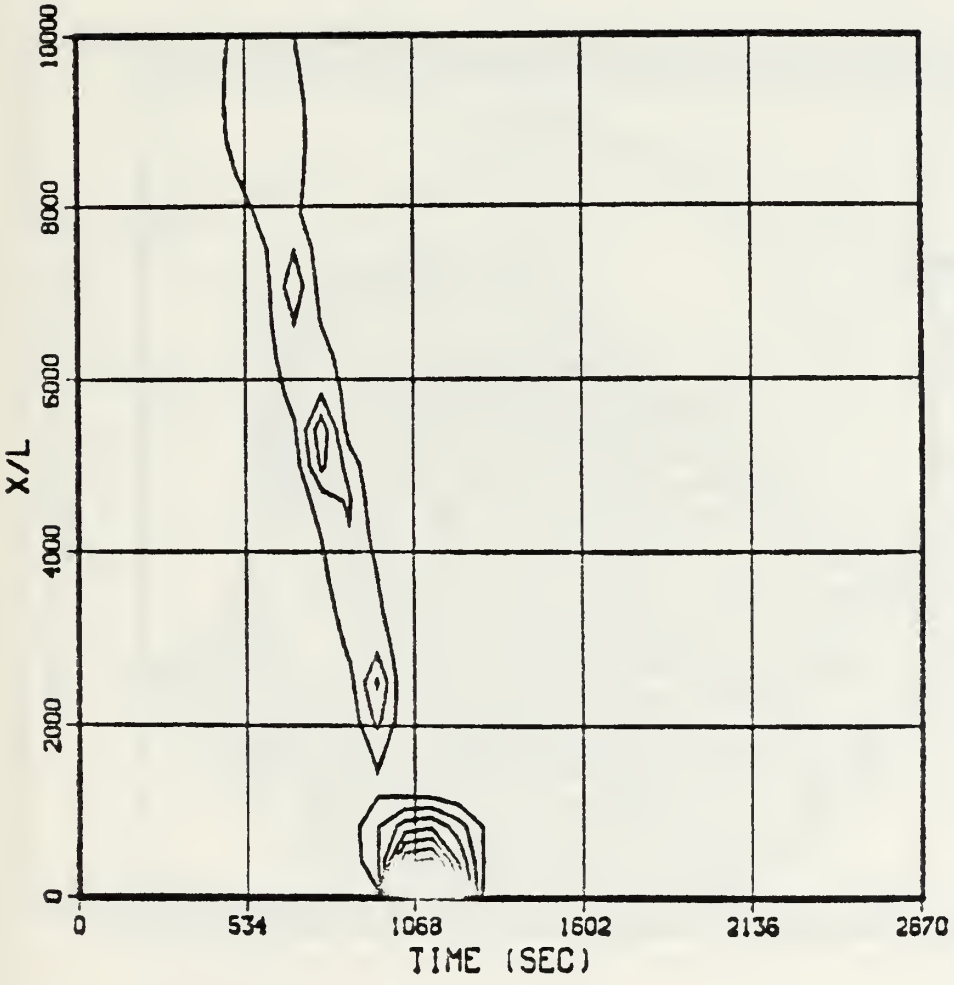


Figure 20. Reaction Rate Contours from GRAF3D

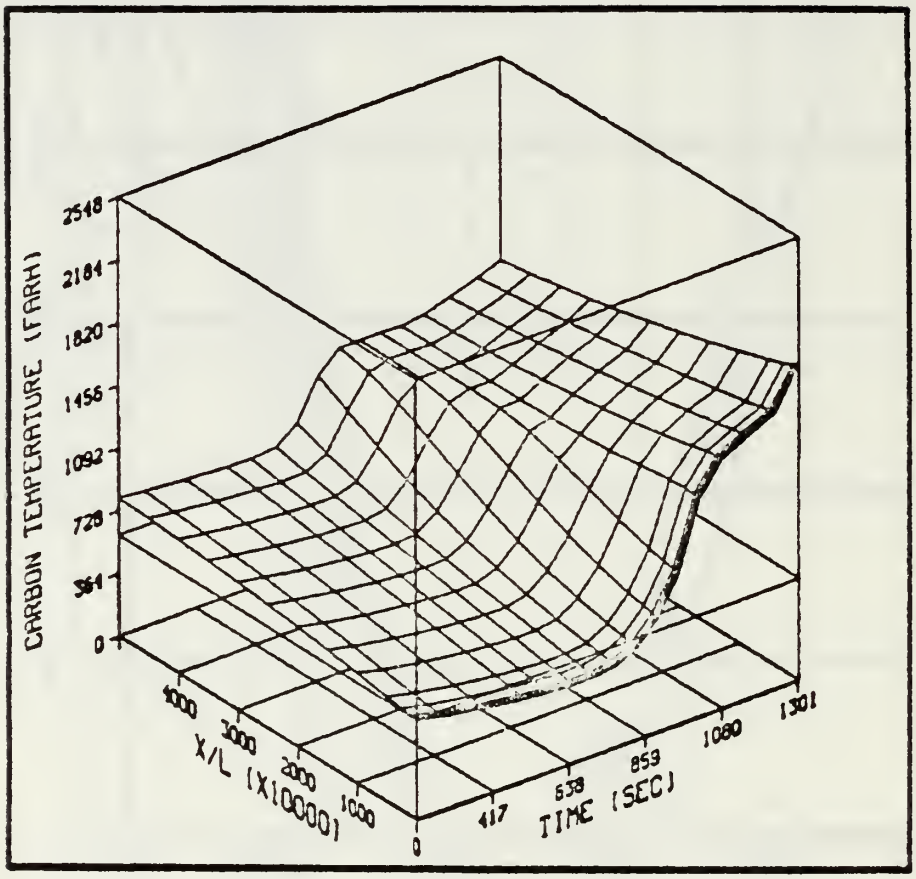


Figure 21. Subregion Surface of Figure 15

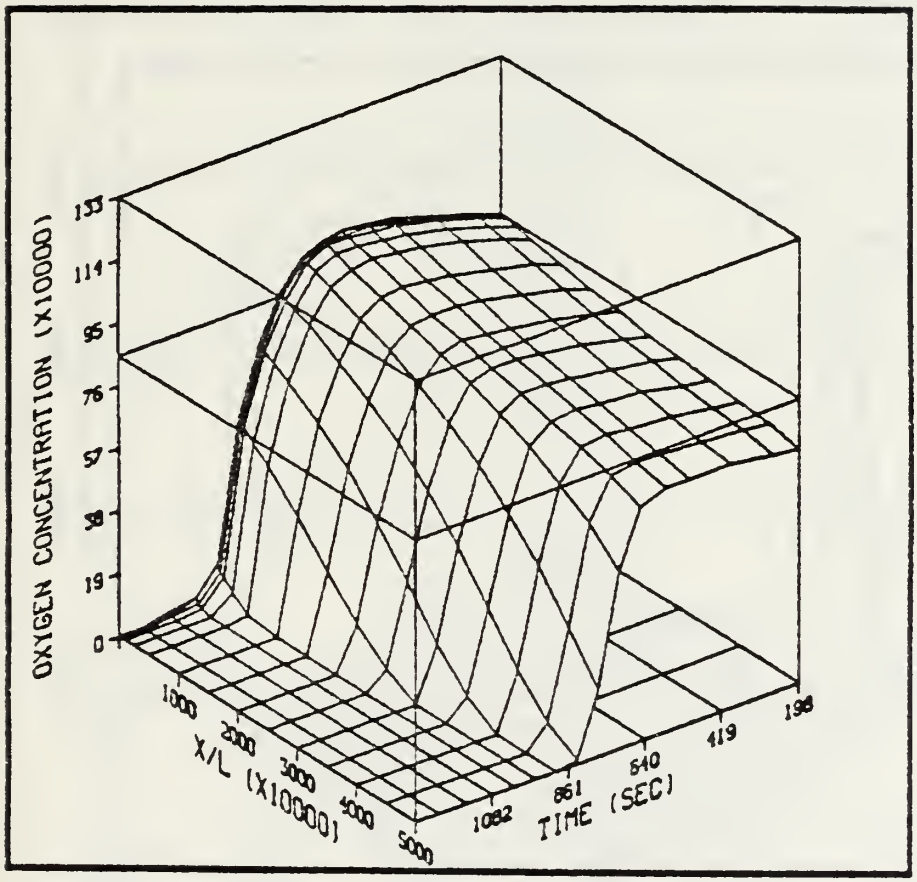


Figure 22. Subregion surface of Figure 16

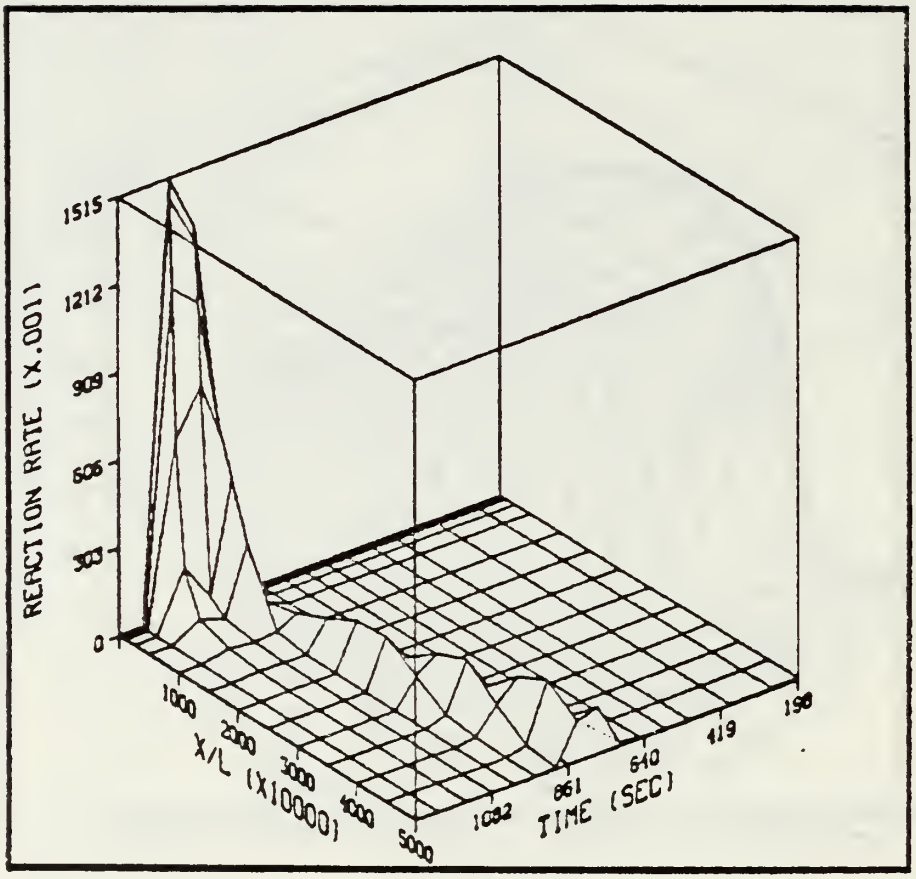


Figure 23. Subregion Surface of Figure 17

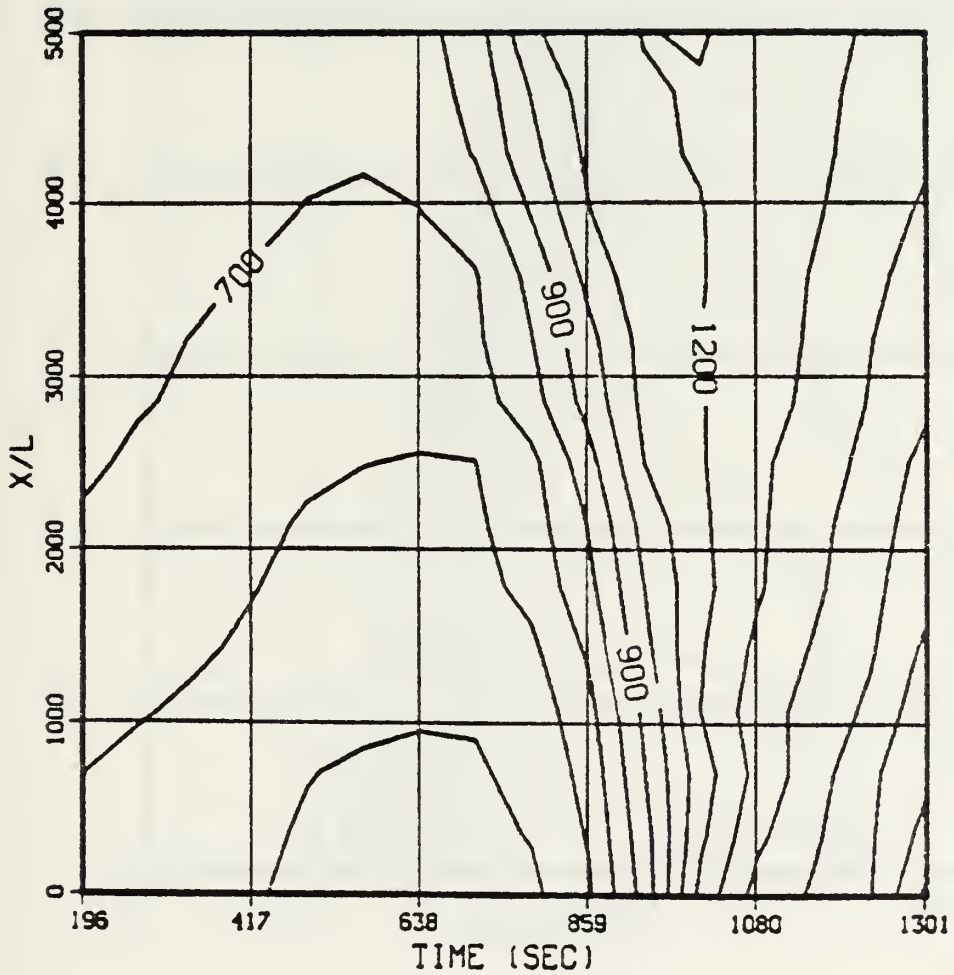


Figure 24. Subregion Contour of Figure 18

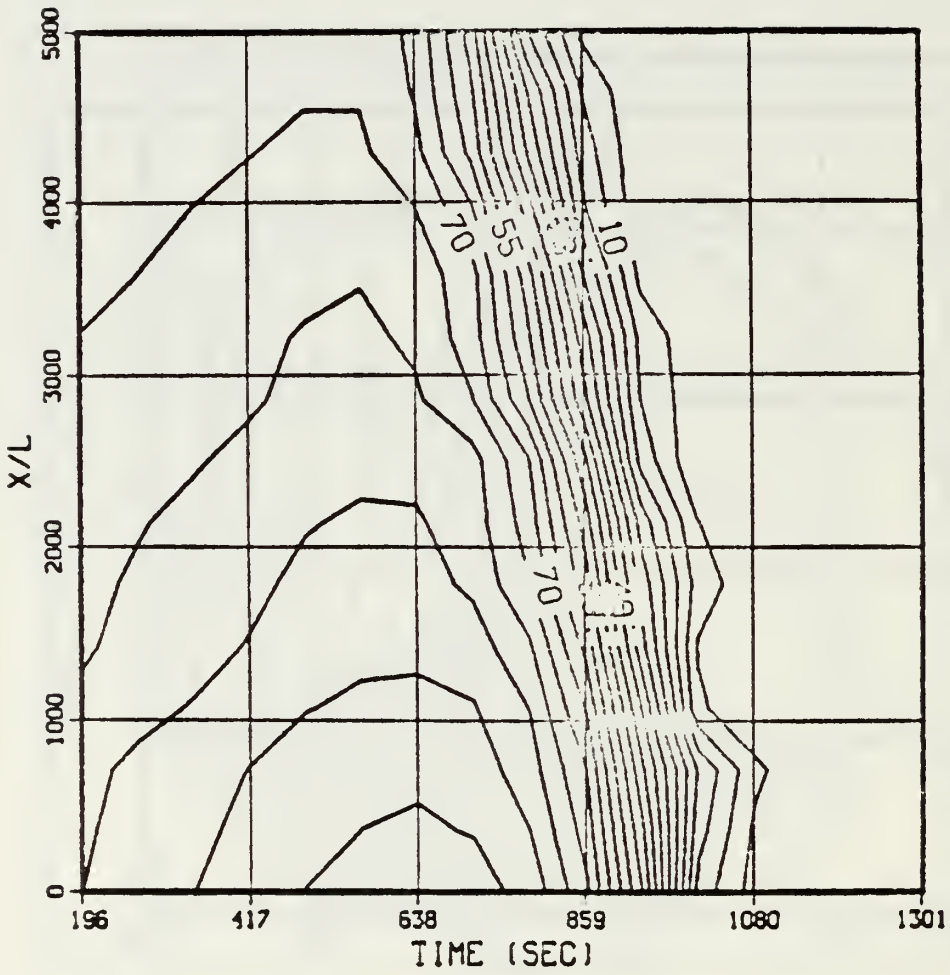


Figure 25. Subregion Contour of Figure 19

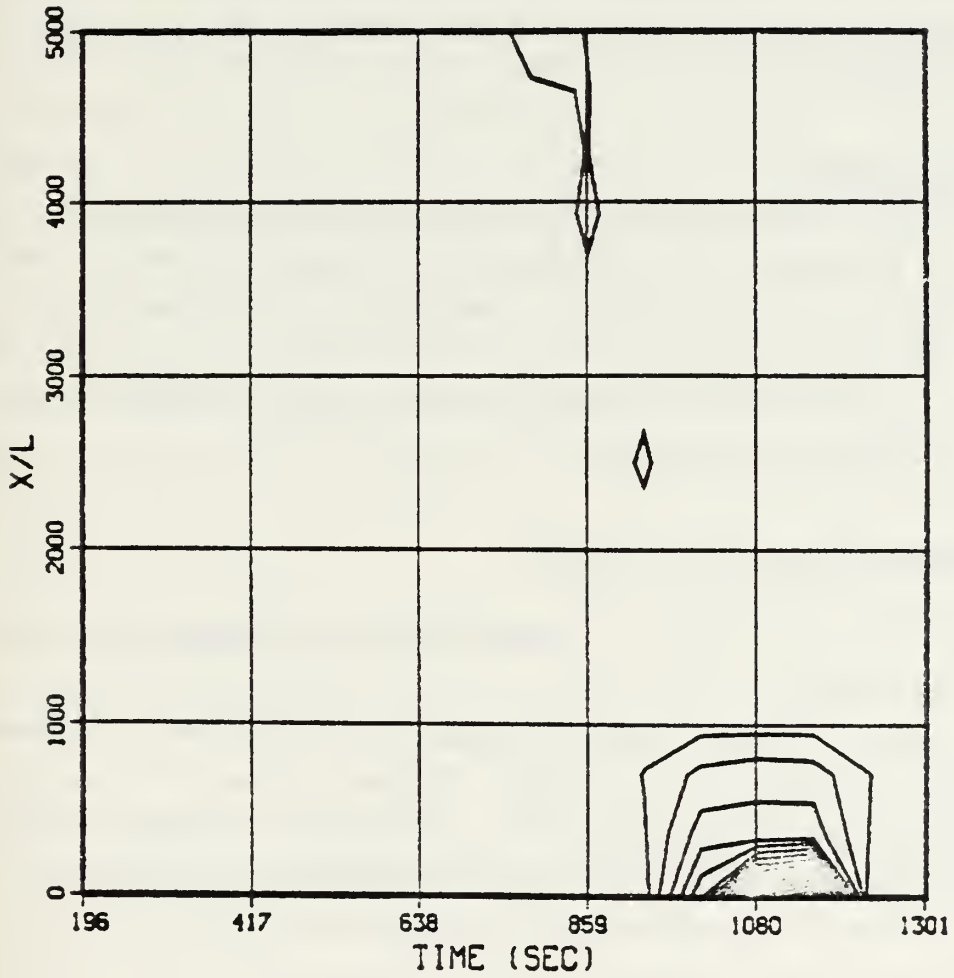


Figure 26. Subregion Contour of Figure 20

# chapter 3
# STRENGTH INVESTIGATION

When a composite laminate is subjected to a thermal distribution, thermal stresses will arise if thermal expansion is restrained. The stresses in a laminate are the result of thermal and load stresses. The strength of a laminate depends upon the stress state and the failure criterion governing failure.

## 3.1 OBJECTIVES

The objectives of the strength investigation are:

1. to determine the stresses in a laminate due to any combination of inplane loads, bending loads, and "thermal loads",
2. to determine the strength of a laminate resulting from these stresses.

## 3.2 DESCRIPTION OF THE MODEL

A detailed formulation and description of the mathematical model is presented in a technical report (8). A brief summary follows.

The model is restricted to symmetric laminates. This is hardly a limitation on the model because

1. nonsymmetric laminates are extremely uncommon, and
2. symmetric geometry does not restrict the model to symmetric temperature distributions.

The formulation begins with the formation of the stiffness matrix of a lamina in the natural coordinates of the lamina. The stiffness matrix of a laminate is obtained from the lamina stiffness matrices by coordinate transformations from the natural axes of a lamina to the laminate coordinate system. These are the laminate stress-strain relations.

The strain-displacement relations (Kirchhoff-Love theory) of thin plate theory are combined with the stress-strain re-

lations to give the laminate force-displacement relations. The stresses in each lamina can be obtained from the forces through the force-stress relations. Temperature effects enter into the analysis through the stress-strain relations, which in turn produced "thermal load" terms in the force-stress relations.

Once the lamina stresses are known, the task is to determine which, if any, of the lamina have failed. The generalized Tsai-Wu criterion is used as the failure criterion for the lamina. The failure of one or more lamina does not imply that the laminate has failed. The strength analysis determines the ply by ply sequence of failure. After a ply (lamina) has failed, the ply is removed, and the stress-strain relations for the modified laminate are generated. This process is repeated until all lamina have failed. If all of the plies have failed, the laminate has failed. If the loading and temperature are such that all of the lamina have not failed, then the laminate has not failed. In this case the task is to determine "how far" the laminate is from failure. This is obtained from calculating the "load factor".

## 3.3 MODIFICATIONS OF THE MODEL

The original formulation of the model was restricted to symmetric temperature field problems. In addition, the analysis was restricted to problems for which only the load factor could be determined. These restrictions have been eliminated in the present model of the strength analysis program (STREN).

### 3.3.1 Nonsymmetric Temperature Fields

The strength analysis program (STREN) was modified to handle nonsymmetric temperature distributions which result, for example, when one surface of the laminate is exposed to a fire. Some of the equations presented in reference (8) are changed as follows:

### 3.3.2 Additional Failure Factors

In it's earlier form, STREN provided the load factor to failure for a specified temperature distribution. The program was modified to handle "temperature factor", and "combined factor" problems as well. each of these problems will be briefly described.

In the load factor problem, the magnitude of temperature in each ply is specified explicitly, and the relative magnitudes of the laminate forces and bending moments are given. If the laminate load vector (Nx,Ny,Nxy,Mx,My,Mxy) is specified as (1.,.5,0.,0.,10.,0.), and the load factor is determined to be R, then for the given temperature field, the laminate will fail when Nx=1.xR, Ny=0.5xR, Nxy=0.xR, Mx=0.xR, My=10.xR, and Mxy=0.xR. Reference (8) shows that the load factor appears as the scalar multiplier of the "load stresses".

In the temperature factor problem, the laminate load magnitudes are specified exactly, and only the relative magnitudes of the ply temperatures are known. In this case, the problem is to determine the factor which when multiplied by the relative lamina temperatures gives the temperature field at laminate failure.

Finally, we consider the combined factor problem. Here the relative magnitudes of both the loads, and ply temperatures are specified, and the task is to determine the "combined factor" which, upon multiplication with each of the relative loads and temperatures, gives the loads and temperatures at which the laminate will fail.

In each case, the Tsai-Wu failure criterion reduces to the quadratic in the factor R,

$$\alpha R^2 + \beta R + \gamma = 0$$

The coefficients $\alpha$, $\beta$, and $\gamma$ depend upon which R factor is being determined. In the load factor case, $\alpha$, $\beta$, and $\gamma$, are the a, b, and c of Equations (65) through (67) of reference (8), respectively. In the temperature factor case, $\alpha$ is b, $\beta$ is a, and $\gamma$ is c. In the combined factor case,

$$\alpha = a + b - F_x(\sigma_{Lx} + \sigma_{Tx}) - F_y(\sigma_{Ly} + \sigma_{Ty})$$

$$\beta = F_x(\sigma_{Lx} + \sigma_{Tx}) - F_y(\sigma_{Ly} + \sigma_{Ty})$$

$$\gamma = -1.$$

### 3.4 SAMPLE ANALYSES

Reference (8) presents some results of the strength investigation. Those results showed good agreement with previous analyses in the literature. The present version of STREN was used to generate a failure locus of a 0/90 graphite-epoxy laminate at a temperature of 200 F below the curing temperature; for all stress states of the form (Nx,Ny,Nxy,Mx,My,Mxy)=(Nx,Ny,0,0,0,0,0,). Since there are only two non zero stress components (Nx and Ny), the locus of failure stress states can be shown as a curve in Nx-Ny space. This curve is shown in Figure 15. This failure locus was generated by running STREN for 37 combinations of Nx and Ny ( i.e., (Nx,Ny) = (1.,0.), (1.,.5),...,etc.).

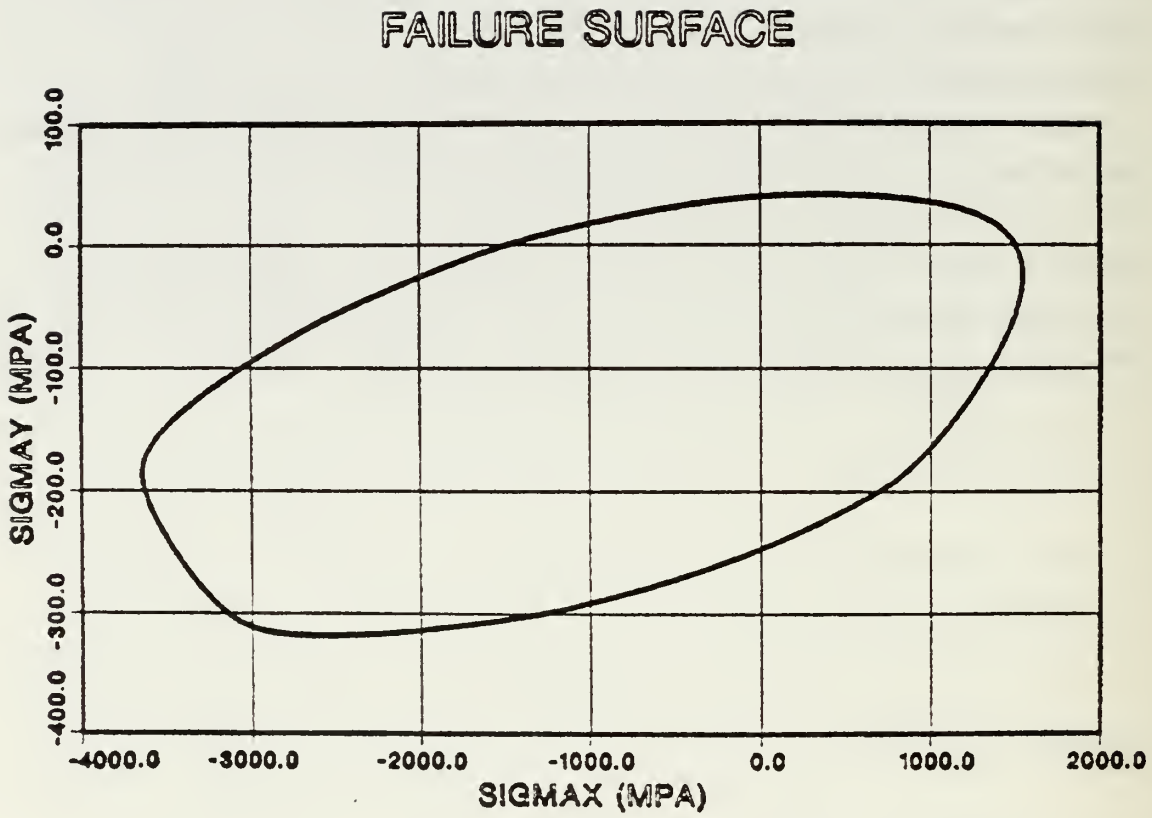


Figure 27. Failure Locus for 0/90 Graphite-Epoxy Laminate

## REFERENCES


1. Fontenot, J. S., "Graphite-Epoxy Composite Material Response to Carrier Deck Fire," Naval Weapons Center, NWC Technical Memorandum 3351, November, 1979.
2. Vatikiotis, C. S. and Salinas, D., "Heat Transfer in a Fibrous Composite with Combustion," presented at the Joint ASME/AIChE National Heat Transfer Conference, Orlando, Florida, July 27-30, 1980, ASME publication 80-HT-108.
3. Vatikiotis, C. S., "Analysis of Combustion and Heat Transfer in a Porous Graphite Medium," Mechanical Engineer's Thesis, Naval Postgraduate School, Monterey, June, 1980.
4. Franke, R., "A Program for the Numerical Solution of Large Sparse Systems of Algebraic and Implicitly Defined Stiff Differential Equations," Naval Postgraduate School Report NPS-53Fe76051, 1976.
5. Vatikiotis, C. S., "A Combustion and Heat Transfer Model for Porous Media," Doctoral Dissertation, Naval Postgraduate School, June, 1982.
6. Frank-Kamenetskii, D. A., "Diffusion and Heat Transfer in Chemical Kinetics," Plenum Press, New York, 1969.
7. Kolodstev, K. H., "Dynamics of Gas Formation in a Carbon Layer," Moscow ZHURNAL FIZICHESKOY KHIMII, Vol.XIX, No.9, pp.417-428, 1945.
8. Salinas, D., "Strength Analysis of Composite Plates in a Thermal Environment," Naval Postgraduate Report, NPS-69-81-005PR, September, 1981.

## Distribution List

| | | Copies |
|---|---|---|
| 1. | Library, Code 0142<br>Naval Postgraduate School<br>Monterey, California 93940 | 4 |
| 2. | Dean of Research, Code 012<br>Naval Postgraduate School<br>Monterey, California 93940 | 2 |
| 3. | Department of Mechanical Engineering, Code 69 | |
| | Professor P. Marto | 2 |
| | Professor G. Cantin | 1 |
| | Professor R. Newton | 1 |
| | Professor G. Vanderplaats | 1 |
| | Professor M. Kelleher | 1 |
| | Professor Y. Shin | 1 |
| | Professor D. Salinas<br>Naval Postgraduate School<br>Monterey, California 93940 | 10 |
| 4. | Professor R. Franke, Code 57<br>Department of Mathematics<br>Naval Postgraduate School<br>Monterey, California 93940 | 1 |
| 5. | Lcdr. C. S. Vatikiotis<br>Carderock Laboratory<br>DW Taylor, NSRDC<br>Bethseda, MD 20084 | 10 |
| 6. | Commander<br>Naval Weapons Center | |
| | Mr. Kent Farmer, Code 3383 | 15 |
| | Mr. John Fontenot | 1 |
| | Mr. J. McManigal<br>China Lake, California 93555 | 1 |
| 7. | Dr. Stephen W. Tsai<br>Wright Patterson AFB<br>Air Force Materials Laboratory<br>Dayton, Ohio 45433 | 1 |
| 8. | NASA Ames Research Center | |
| | Mr. Joseph Mansfield, Code 223-6 | 1 |
| | Mr. Dick Fish, Code 223-6<br>Mcffitt Field, California 94035 | 1 |